SMACS MODEL – A Stochastic Multihorizon Approach for Charging Sites Management, Operations, Design, and Expansion under Limited Capacity Conditions

CenSES Working Paper 1/2019

07 February 2019

Chiara Bordin, Asgeir Tomasgard

ISBN: 978-82-9319 8-29-1

CenSES
Centre for Sustainable Energy Studies

NTNU – Trondheim
Norwegian University of Science and Technology

SMACS MODEL

A Stochastic Multihorizon Approach for Charging Sites Management, Operations, Design, and Expansion under Limited Capacity Conditions

Chiara Bordin[1], Asgeir Tomasgard[2]

[1] Sintef Energy Research, Trondheim - Norway

Energy Systems Department

[2] Norwegian University of Science and Technology, Trondheim - Norway

Department of Industrial Economics and Technology Management

chiara.bordin@sintef.no, asgeir.tomasgard@ntnu.no

Abstract

The increasing demand of electric vehicles creates challenges for the electric grid both on the transmission level and distribution level. Charging sites in particular will have to face strong challenges especially in those countries where a massive penetration of electric vehicles happened in the last years and even more is expected in the forthcoming future. Such an increased forecast demand will lead to a capacity lack within the existing charging sites, therefore new investments in design and expansion have to be planned. We propose the so called SMACS MODEL that stands for Stochastic Multihorizon Approach for Charging Sites Management, Operations, Design and Expansion under Limited capacity conditions. The model is built to analyse critical decisions in terms of transformer expansion, grid reinforcements, renewable installation and storage integration, over a time horizon of ten years, with a particular focus on the long term uncertainty in the price variations of the available resources. Long term investment decisions and short term operational decisions are addressed simultaneously in a holistic approach that includes also battery degradation issues and is able to tackle the optimal trade off between battery replacements, grid reinforcements and renewable installations throughout the chosen time horizon. Compared to traditional decision approaches the model is able to take more precise decisions due to its higher insight on the long term costs projections, the inclusion of battery degradation issues and the inclusion of grid rules and regulations limits that affect the final decisions.

Keywords: electric vehicles, stochastic optimisation, multihorizon, charging sites, battery degradation, design, expansion

Table 1: Nomenclature - Parameters

Renewable	
R	unitary current investment cost of the renewable plant (\$)
R_n^L	long term multiplier that defines variations in the renewable investment costs in every strategic node n
R^{eff}	efficiency of the renewable plant of type w (%)
$R_{t,p,s}^{\beta}$	forecast production of one unit of renewable source in time t, profile p, operational scenario s (kWh)
R^{lim}	upper limit in the possible renewable installation linked to available area (kWh)
Transformer	
T_i	current investment cost of the transformer of type i (\$)
T_n^L	long term multiplier that defines variations in the transformer investment costs in every strategic node n
T_i^{eff}	efficiency of the transformer of type i (%)
T_i^{cap}	capacity of the transformer of type i (kVA)
F	power factor for the conversion from kVA to kW (%)
$\widehat{T}_i^{cap}$	capacity of the existing transformer of type i (kVA)
$T^{\%}$	percentage of the peak demand that limits the transformer capacity increment in every strategic node (%)
T^{lim}	upper bound on the maximum size allowed for a distribution transformer (kVA)
Battery	
B_j	current investment cost of the battery of type j (\$)
B_n^L	long term multiplier that defines variations in the battery investment costs in every strategic node n
B_j^{eff}	efficiency of the battery of type j (%)
B_j^{cap}	capacity of the battery of type j (kWh)
B_j^{ch}	minimum state of charge of the battery of type j (%)
B_j^{rt}	rating of the battery of type j (%)
B^{init}	desired state of charge of the battery at the beginning of every typical profile (%)
B^{fin}	desired state of charge of the battery at the end of every typical profile (%)
B_j^{thr}	lifetime throughput of battery of type j (kWh)
B_j^{fade}	capacity fade of battery of type j when 100% of the total throughput is used (%)
Demand	
$D_{t,n,p,s}$	forecast demand in time step t, profile p, operational scenario s within strategic node n (kWh)
D_n^L	long term multiplier that defines demand variations in every strategic node n
$D_{t,p,s}^{\beta}$	short term multipliers modelling the daily demand trend in time t, profile p, operational scenario s
D_n^{peak}	peak demand in every strategic node n (kWh)
Electricity Price	
$P_{t,n,p,s}$	forecast electricity price in time step t, profile p, operational scenario s, within strategic node n (\$/kWh)
P_n^L	long term multiplier that defines price variations in every strategic node n
$P_{t,p,s}^{\beta}$	short term multipliers modelling the daily price in time t, profile p, operational scenario s
Grid Reinforcement	
G^{cost}	unitary cost of digging for cable installation (\$/km)
G^{cab}	unitary cost of cables (\$/km)
G^{cap}	cable capacity (amps)
k	distance of the charging site from the transformer substation (km)
H	factor for converting amps to kW in cable sizing
$G^{\%}$	percentage of additional transformer capacity at which grid reinforcement will occur (%)
Other	
P_s	probabililty of operational scenario s (%)
P_n	probabililty of strategic node n (%)
Y_n	year number associated to strategic node n
ω_p	weight of profile p
r	interest rate (\$)
$BigM$	a very big number

Table 2: Nomenclature - Sets and Indexes

Sets and index	
$t \in \mathcal{T}$	set of operational time periods
$p \in \mathcal{P}$	set of operational profiles
$n \in \mathcal{N}$	set of strategic nodes
$s \in \mathcal{S}$	set of operational scenarios
$j \in \mathcal{J}$	set of battery types
$i \in \mathcal{I}$	set of transformer types

Table 3: Nomenclature - Variables

Variables	
$f^{RD}_{t,n,p,s}$	energy flow from the renewable plant to the demand in time t of strategic node n for profile p, operational scenario s (kWh)
$f^{RB}_{t,n,p,s,j}$	energy flow from the renewable plant to the battery j in time t of strategic node n for profile p, operational scenario s (kWh)
$f^{TD}_{t,n,p,s,i}$	energy flow from the transformer i to the demand in time t of strategic node n for profile p, operational scenario s (kWh)
$f^{TB}_{t,n,p,s,i,j}$	energy flow from the transformer i to the battery j in time t of strategic node n for profile p, operational scenario s (kWh)
$f^{BD}_{t,n,p,s,j}$	energy flow from the battery j to the demand in time t of strategic node n for profile p, operational scenario s (kWh)
$\theta_{n,i}$	integer variable defining the units of transformer of type i installed on strategic node n
$q^{T}_{n,i}$	variable that keeps track of the actual installed transformer capacity in every strategic node n
z	cable size that can accomodate the transformer capacity (amps)
$\theta_{n,j}$	binary variable equal to 1 if the battery of type j is installed on strategic node n
$\varepsilon_{n,j}$	integer variable defining the number of batteries of type j to be installed on strategic node n
$q^{B}_{n,j}$	variable that keeps track of the actual installed battery capacity in every strategic node n
$b^{SOC}_{t,n,p,s,j}$	state of charge of the battery j in every time step t of strategic node n for profile p, operational scenario s (kWh)
$y_{t,n,p,s,j}$	binary variable equal to 1 if the battery of type j is charging in time t of strategic node n for profile p, operational scenario s
λ^{R}_{n}	continuous variable defining the additional renewable capacity to install in the strategic node n (kW)
q^{R}_{n}	variable that keeps track of the actual installed renewable capacity in every strategic node n (kW)
g_n	binary variable equal to 1 if grid reinforcement is needed on strategic node n
c^{REF}_{n}	transformer reference capacity in very node n used to decide if grid reinforcement is needed (kVA)
$h^{INIT}_{n,j}$	residual lifetime throughput of battery of type j at the beginning of the strategic period n (kWh)
$h^{FIN}_{n,j}$	residual lifetime throughput of battery of type j at the end of the strategic period n (kWh)
$b^{REP}_{n,j}$	binary variable equal to 1 if a battery replacement of type j occurs on strategic node n
$h^{REP}_{n,j}$	battery residual throughput that is still available in the old battery once the replacement occurs (kWh)

1 Introduction

The increasing demand of electric vehicles creates challenges for the electric grid both on the transmission level and distribution level. Charging sites for several vehicles will in particular face challenges due to its potentially high maximal power consumption. Here it is not the energy consumption that is challenging, but the fact that the maximum capacity in the distribution network and station itself is limited. This motivates to study the problem of smart design and operation of charging sites. In the short run, the existing capacity at the charging site must be allocated efficiently, also limited by the local distribution grid. Clearly, the regime for operating the charging site will also strongly affect the design and capacity need. In the long run the design of the site in terms of capacity, location and interplay with the rest of the power system addresses the trade-off between costs for investments in new grid capacity and the service level of the charging station. Here typical design elements can be the charging capacity, local power generation capacity, the capacity of batteries installed to smooth out the residual load, transformer capacity as well as potentially the need to increase the dimension on the distribution grid. The main objective of our paper is to show under which conditions storage integration and renewable integration becomes convenient compared to grid reinforcement investments.

In this paper we propose to address this problem of integrated planning of operations, design and capacity expansion by using a multistage stochastic programming approach. For this purpose we develop an integrated model for design and operation, a Stochastic Multihorizon Approach for Charging Sites Management, Operations, Design and Expansion under Limited capacity conditions (SMACS MODEL). This model is used to analyse critical decisions in terms of transformer expansion, grid reinforcements, renewable installation and storage integration, over a time horizon of ten years. There is a novel focus on the long-term uncertainty in the price variations of the available resources and cost development: long-term investment decisions and short-term operational decisions are addressed simultaneously in a holistic approach.

The main contribution is the methodology to handle the trade-off between battery replacements, grid reinforcements and renewable installations throughout the chosen time horizon based on stochastic modelling. The multistage stochastic model includes both short-term and long-term uncertainty. The model framework is tested on realistic data, and results has been analysed to discuss the value of a multihorizon perspective versus traditional approaches that are usually neglecting learning effects and uncertainty in investment costs.

Moreover, a second contribution is a detailed methodology to include battery technical properties and degradation in order to optimise battery stock replacements throughout the years according to residual lifetime throughput and capacity degradation.

A third contribution is the extensive computational experiments and sensitivity analyses with real world dataset that has been performed. We provide real world dataset related to the cost

projection of different energy technologies, as well as electricity price and demand forecast development. Analysis are performed to investigate the trade-off between performance and costs over time. A particular focus has been put on investigating which combinations of storage replacement costs and grid reinforcement costs make the system economical under different demand assumptions. Further tests have been done to investigate the trade-off between cheaper batteries with lower performance and more expensive batteries with better performance.

The study shows that the ability to take decisions by considering the uncertainty in the future development of investment costs of energy units is crucial. Technology improvement drastically affect the timing, cost and performance of the charging site.

The structure of the paper is as follows: Section 2 will present a literature review in the field of charging sites operations, location-allocation and design; Section 3 will introduce the main technical aspects linked to battery properties, transformer properties and grid reinforcement tasks that are needed to understand the mathematical model presented in the following Section 4; the real world data set used for computational experiments will be discussed in Section 5 while testing and results will be presented in Section 6; finally, Section 7 will draw the conclusions.

2 Literature Review

A few optimization approaches related to charging sites exist in the literature. We divide them into the following categories: charging site operation, charging site location-allocation and charging site design.

Charging site operation regards the problem of managing the local resources like batteries and available charging capacity (power) in shorter time horizons (often decided by the charging cycle of the batteries). A comprehensive review on scheduling methods for charging sites is proposed in [1] where conventional optimisation methods, game theory and heuristcs algorithms are surveyed. A review and classification of method for smart charging of electric vehicles for fleet operators is presented also in [2]. A framework for optimizing charging and discharging of the electric drive vehicles, given the driving patterns of the fleet and the variations in market prices of electricity is presented in [3]. Moreover, a novel optimal charging scheduling strategy for different types of electric vehicles is proposed in [4] where analyses are based not only on transport system information, such as road length, vehicle velocity and waiting time, but also grid system information, such as load deviation and node voltage. An optimization framework for the operating model of battery swapping stations is proposed in [5] while a model which yields the rate of degradation of the battery as a function of both temperature and depth-of-discharge is proposed in [6]. The latter is then used in an electric vehicle energy management optimization problem, where the degradation suffered by the battery due to a controlled charge is minimized. In [7] authors present a model dealing

with the simultaneous scheduling of electric vehicles and responsive loads to reduce operation costs and emissions in presence of wind and photovoltaic sources in a microgrid. Renewable sources are included also in [8] where a two-stage framework for the economic operation of a microgrid-like electric vehicle parking deck with on-site photovoltaic generation is presented.

Charging site location-allocation problems are oriented towards the problem of locating in a geographical area a set of charging stations, and simultaneously deciding their capacity based on allocation of customers demand to each site. An optimisation approach for charging stations location is proposed in [9]. This paper proposes a new location model based on the set cover model taking the existing traditional gas station network as the candidate sites to determine the distribution of the charging and battery swap stations. An Integer Linear Programing approach for siting and sizing of electric taxi charging stations is proposed in [10]. A queueing model is adopted to estimate the probability of taxis being charged at their dwell places. Input guiding the location and capacity decisions comes from large-scale GPS trajectory data collected from the taxi fleet. The optimal planning of electric vehicles charging/swap stations with MILP approach is proposed in [11]. Here models for location and capacity decisions are developed for rapid-charging stations and battery swap stations considering the distribution network and potential reinforcement. In [12] the charging station location problem includes where to locate the charging stations and how many chargers should be established in each charging station. In [13] the authors present an analytical approach to estimate the optimal density of charging stations for certain urban areas, which are subsequently aggregated to city level planning. In [14] a multi-period model for strategic charging station location planning is presented, recognizing that CS will be introduced gradually over time. A study based on the real traffic flow data of the Korean Expressway network is presented.

These studies focus on location of multiple charging stations in big regions rather than design and expansion of particular charging sites. The charging site design problem addresses the more detailed design and capacity planning of a single site and investigates the optimal capacity based on deterministic or stochastic demand for charging services. If the model includes long-term dynamics so that investment decisions can be optimally timed we call it a design and expansion problem. In both cases the models include dimensioning of technical equipment like maximum charging power, local generation, transformers, batteries and local grid may be included. The charging site design problem is addressed in [15] through a simulation approach that makes use of the HOMER simulation software, and in [16] where authors proposed an algorithm for the optimal sizing of different units, but the uncertainty in prices and production both on the short term operational level and on the long term strategic level is not considered. In [17] authors present an approach that considers time and distance from electric vehicles to a charging station as well as construction costs of transformers, cables, chargers and operational grid (harmonic power loss and other) to determine the optimal placement and sizing of charging stations.

Our contribution is on the charging station design and expansion problem including the integration with the grid. We consider both local RES production, batteries and transformers to balance the capacity of the CS with the distribution system costs. In order to provide the needed detail for the capacity planning, representative operational time periods are added. A novel approach combining short-term uncertainty in the operational horizon (i.e. load, generation) and long-term uncertainty (i.e. cost development) is used. To make this computationally tractable we use multihorizon stochastic programming. As far as the authors know, this is the first approach where the long-term design decisions are linked to this detail level on the operational level for charging site design including stochasticity in both the long run and short run.

While there is no literature on this for charging sites, the general literature on capacity expansion suggests that detailed modelling of short-term dynamics and stochasticity is a necessary approach. Below we give some examples on stochastic capacity expansion and multihorizon stochastic programming respectively. The stochastic capacity expansion problem is a well known and extensively studied. A three level MILP approach is proposed in [18] where optimal expansion of an electric network with demand uncertainty is proposed using an equilibrium model. A real application in the power system in Chile is presented. A stochastic methodology for capacity expansion planning for remote microgrids is presented in [19] where uncertainty is addressed with Monte Carlo approach and authors aim at investigating the economic benefits of including uncertainty in such kind of problems. Although operational uncertainty is considered, long term investment uncertainty is not taken into account, especially regarding different technologies investment prices. A stochastic multistage methodology is used also in [20] for transmission expansion planning and energy storage integration. Although the methodology is multistage with a longer time horizon, the uncertainty in the investment costs of energy units such as storage and renewables is not addressed, only operational uncertainty. A main issue with stochastic capacity expansion problems is the joint modelling of dynamics and stochasticity. Long-term dynamics is the process of repeated investment decisions in several time periods, hence the possibility to time investments. Short-term dynamics is the development of decisions in operational time periods where renewable energy sources generation, load and batteries are managed over a sequence of hours and/or days. When combining these dynamics with long-term uncertainty (costs development, demand trends) and short-term uncertainty (load, generation) in a stochastic programming model, the size of the scenario trees grows exponentially. Multihorizon stochastic programing is a modelling framework developed in particular to address this issue [21]. The main idea is that as long as the future long-term outcomes of stochastic variables are not linked to the history of the short-term uncertain variable outcomes, the long-term development can be separated from the short-term stochastic process using local end-of-horizons operationally. The main real world applications of multihorizon models found so far in literature are related to hydro plants management and load management in buildings. The

first use was in modelling natural gas infrastructure development under uncertainty as shown in [22] and [23]. Another application is hydro power planning where [24] and [25] compare multihorizon models with alternative state-of-the-art modeling approaches. The method has been used in a TIMES energy system model to study short-term uncertainty in RES generation and its effects on the energy system design ([26] and [27]). Skar et al uses a multihorizon approach in EMPIRE, a stochastic model for the European power system ([28]). Moreover, the multihorizon methodology is used in [29] to analyse retrofitting opportunities for energy-efficient buildings on a long-term horizon by taking into account uncertainty in energy prices and technology costs stemming from deregulation.

To our knowledge this is the first attempt to handle both short-term and long-term dynamics and uncertainty in optimal charging site design and expansion.

3 Background on technical aspects: Batteries, Transformers and Grid Reinforcement

This section will give a broad overview of the main technical aspects linked to battery properties, transformer properties and grid reinforcement tasks. The objective is to outline the main features that needs to be taken into account when building mathematical optimisation models for the design and expansion of sites that are supposed to contain such technologies. This will provide a broad overview and an essential introduction that will facilitate the understanding of the technical constraints that are part of the mathematical model proposed in the following section.

3.1 Batteries Technical Notes

Batteries are rated in terms of their nominal voltage and ampere-hour capacity (Ah). Assuming that the voltage is constant and equal to the nominal voltage, the battery capacity B_j^{cap} given in kWh can be calculated as the battery voltage multiplied by the Ah. The roundtrip efficiency B_j^{eff} indicates the percentage of the energy going into the battery that can be extracted later. We assume that the efficiency in both directions is the same (see [30] and [31]). The minimum state of charge B_j^{ch} defines a limit below which a battery must not be discharged to avoid permanent damage.

The so called C-rate (B_j^{rt} in the nomenclature) defines the rate at which a battery is being discharged. It is defined as the ratio between the discharge current and the theoretical current under which the battery would deliver its nominal rated capacity in one hour. A 1C discharge rate means the battery is able to deliver the entire capacity in 1 hour. While a 2C discharge rate means the battery is able to discharge twice as fast (hence it will deliver the entire capacity in 30 minutes).

The state-of-charge of a battery is the percentage of its capacity available relative to the capacity when it is fully charged. By this definition, a fully charged battery has a state-of-charge of 100% and a battery with 20% of its capacity removed has a state-of-charge of 80%.

For further readings about battery properties we refer to [32] and [33].

3.1.1 Battery Degradation

The life of a battery can be measured by the so called *lifetime throughput* B_j^{thr} that defines the total amount of energy in kWh that can be discharged before it is no longer able to deliver sufficient energy to satisfy the load requirements of the system. The lifetime curve provided by manufactures relate different depth of discharge with the number of residual cycles to failure. The deeper the discharge, the lower the number of related cycles to failure [34].

The state-of-health of a battery is the percentage of its capacity available when fully charged relative to its rated capacity. For example, a battery rated at 30 Ah, but only capable of delivering 24 Ah when fully charged, will have a state-of-health of 24/30* 100 = 80%. Thus, the state-of-health takes into account the loss of capacity as the battery ages. Through the lifetime throughput calculation, manufactures guarantee that the capacity of the battery will not drop more than a certain percentage B_j^{fade} as long as the total energy drawn is kept within the lifetime throughput. Therefore, at the end of life, if 100% of throughput has been used, it is reasonable to expect that the battery capacity will not be lower than a certain percentage (usually 20%). Academic battery literature has typically considered a battery degraded to the point of needing replacement when it is only able to provide 80% of its original capacity [35]. Hence it is reasonable to expect a remaining capacity around 80% when the battery throughput is finished and the battery reaches the end of life.

3.1.2 Battery Bank Upgrade

In a battery bank mixing batteries of different ages is not recommended as they interact with each other. The overall performance is only as good as the weakest link in the chain [36]. Unfortunately, that means when one battery in a bank of two or more batteries needs to be replaced, they should all be replaced at the same time. As discussed in [37] the behavior of batteries during discharging and charging varies throughout their lifespan and if all the batteries are the same age, then they all will have similar responses.

Limitations in battery bank sizing are mainly given by the available space and eventually related costs linked to alternative use of the required area. An (8*20*8) ft container can house 1 MWh lithium ion batteries. It will be necessary approximately four times this size for the same amount of lead-acid or redox-flow batteries. Beyond space, weight limitations can occur as well depending on the particular location and application. Apart from space and weight, there are no particular

limitations to how big a battery storage can be. Among the largest battery installations in the world we find the Mitsubishi storage facility in Buzen, Japan, [38] with 300 MWh capacity (252 containers for a total area of 14000 square meters); Tesla grid storage facility for the Southern California Edison with a capacity of 80 MWh [39]; Escondido substation in California with 120 MWh capacity [40].

3.2 Transformer Technical Notes

A transformer is an electrical device that transfers electrical energy between two or more circuits through electromagnetic induction. In this particular study we refer to step down transformers that will decrease the high transmission line voltage towards lower values suitable for distribution loads such as charging sites.

Due to the magnetic field a transformer will draw both active power (kW) and reactive power (kWAr) from the source. The net result of this two powers is the apparent power (kVA). Hence transformer capacity T_i^{cap} is given in kVA. In order to determine the actual output power in kW it is necessary to know the particular load *power factor* F defined as the ratio of the real power flowing to the load to the apparent power in the circuit. It is a dimensionless number in the interval of 0 to 1. For computational testing purposes it is reasonable to assume a power factor around 0.9 (see for instance datasets discussed in [41] and [42]) which realistically assumes that the voltage and current waveforms are not in phase, reducing the instantaneous product of the two waveforms $(V * I)$.

For further reading about transformers and electric power theory it is possible to refer to [43].

Two main guidelines should be considered when choosing the size of a transformer:

- it should have enough capacity to handle the forecast loads and a certain amount of overload
- it should be possible to increase the capacity to handle future loads increment

Installing a transformer that is too small may cause outages and voltage drops, while installing a transformer that is too large may bring unnecessary load loss. Finding a solution means being aware of transformer losses and overload issues. There are two main types of transformer losses: coil losses (called load losses), and core losses (also called no-load losses).

The coil losses (load losses) originate in the primary and secondary coils of the transformer as a result of the resistance of the winding material.

The core losses originate in the steel core of the transformer as a result of the magnetizing current needed to energize the core. Such losses are constant, they don't depend on the load, and therefore are also known as no-load losses. As long as the transformer is energized, the no-load losses will constantly waste energy. Moreover, such losses increase with the capacity (kVA) of the

transformer: hence proper sizing is crucial and a careful selection of the transformer capacity will ensure lowest core loss.

As stated in [44] the no-load loss is considered as a critical factor as it has undesirable impacts on the aging of transformers. Moreover, oversized transformers can introduce problems such as very high inrush currents, excessive fault levels, higher core losses and a larger footprint [45].

More details about transformer losses and related damaging costs can be found in [46].

It is anyway important to have a transformer bigger than the peak demand to avoid overload that affects negatively the lifetime. The main issue related to overload is heat dissipation. Prolonged periods of transformer overloading causes service life decrements, and in worst-case scenarios, results in tripped thermal relays and residential service outages [47]. If a transformer is overloaded for long period of time, heat will develop internally within the transformer coils and potentially cause serious problems [48]. In fact, the useful life of a transformer is the useful life of the insulating system, and the life of the insulation is related to the temperature being experienced.

Given the above technical details, the transformer capacity upgrade has to be limited to a certain value in order to avoid oversizing issues. Hence as a general guideline a transformer should not exceed the peak demand more than a certain percentage $T^{\%}$. This will put an upper bound on the size to avoid oversizing issues, but at the same time will leave some exceeding capacity to avoid overloading issues. Such limit can vary according to the particular application or rule and regulation of a particular country etc. Sensitivity analyses can be performed to investigate the effect of such limitations in the final optimal system design.

For further reading about transformer proper sizing and selection it is possible to refer to [49].

3.3 Grid Reinforcement Technical Notes

Lines in the distribution grid are oversized to take into account both extreme peak loads and possible future additional needs. When the transformer capacity in the charging station increases to a certain level, the distribution grid supplying the charging station also needs to be strengthened. Of course, such limits can vary according to the particular location, the local grid characteristics and regulations of the particular country. Reinforcement costs for grids will typically occur when the needed capacity is greater than a certain percentage $G^{\%}$ of the existing one.

4 Mathematical Model

The problem addressed in the mathematical model takes as a starting point a location for a charging site and either suggests expansion its existing capacity and suggests an optimal expansion, or does the optimal design for a greenfield installation. The model is dynamic, so the capacity expansion elements is in any case the central element. Given an existing charging site, the need for expansion

will be driven by higher charging demand forecasts. As this is a stochastic model, this future demand may be uncertain along with the cost developments. Investment decisions are hence made under uncertainty.

One of the key characteristics of the model is that we in addition to the long-term uncertainty also model short-term uncertainty that affects the operations directly and the investments indirectly through operational costs. Another key characteristic is the need to balance the capacities in the demand (load), the local generation of renewable energy, the storage capacity (battery), the transformer capacity and the local grid. Both batteries and renewable energy generation reduce the need for grid, but comes at a cost. The effect of these investments depends on the variations in renewable energy generation and load as well as the correlations between these.

The problem is a combination of a design problem and an operational management problem that have to be addressed together. The design choices are affected by both the long-term uncertainty in the solar panels and battery purchase costs as well as the short-term uncertainty in the renewable generation and demand and the resulting operational costs. Clearly also the short-term management of the system is limited by the installed capacities. This is the purpose of using a stochastic multihorizon optimisation model where the main decisions are the long-term investments, but a number of operational representative periods are included to include the expected effects on the operations. The main objective is to minimise the total expected investment and operational costs.

4.1 The Multihorizon Scenario Tree

The information process of the model is shown in Figure 1, depicting a multihorizon scenario tree [21] describing how the uncertainty (both in the short term and long term) is unresolved and the corresponding sequence of decisions when new information is known. Investment decisions in terms of units to be installed are made in strategic nodes (black bullets). A long-term scenario consists of all the strategic nodes on a path from the root node to a leaf. The depicted tree has a two-stage structure where long-term uncertainty is resolved once (at time t=1) and the outcome of all long-term is know at that stage. Of course both a different time for resolving uncertainty, and a multistage structure is supported by the methodology. Each of the long term scenarios show a different development for the investment costs for the various units such as batteries, transformer, renewable plants (black arcs). Six long term scenarios are shown in Figure 1 departing from the root node.

Figure 2 shows the details of short term operational scenarios. In particular, from every strategic node (black bullet), two operational scenarios are shown (red arcs) to take into account the short-term uncertainty in the demand and renewable production. Operational decisions on energy flows are made in operational nodes (blue bullets) that are embedded in every operational scenario. The

operational uncertainty is described in a two-stage tree, where uncertainty is partly resolved in the first branching and completely resolved in the operational leaf nodes, the operational end-of-horizon. Other structures may of course be chosen for the operational tree, based on the need to model the sequence of operational decisions under uncertainty. Examples of such decisions may be flows into and out of batteries and allocation of capacity to chargers.

Figure 2 shows that for every scenario, the operational nodes are split into three different profiles that aim at representing typical periods of the year. Here every short-term scenario is represented by the path from the strategic node to the leaf node. Each period represents a typical week in a year, hence it has to be made of 168 operational nodes, that represents the hours in a week. The number of operational periods, should be decided by the need to capture time correlations and to manage the storage cycles. As we are including battery storage, we need to bear in mind that the state of charge of the storage unit will be defined as input at the beginning of every operational scenario. That is the limitation of the multihorizon trees. No information is passed between two operational periods linked to different strategic nodes. Imposing such state of charge at the beginning of every day would not be a very strong assumption in a strategic model. Remember, this is not a an operational model that will be used for actual operational decisions. The operational periods are there to illustrate the effects of different strategies. Also the normal charge level at the beginning of a week can be considered a long-term decision. Normally the battery will be filled at a time outside the peak capacity hours. After some preliminary tests, it has been found that a weekly length is suitable as the model has the freedom to charge and discharge within seven days without any strong assumption on the daily state of charge.

Note that inside the model every profile will be multiplied by a weight that defines how many times such typical profile occurs in a year. For instance, if we choose daily typical profiles of 24 hours, then the related weights will be: 90 days of winter, 90 days of summer, 185 days for the rest (365 days in a year). For weekly typical profiles of 168 hours, the weights will be defined by 12 weeks of winter, 12 weeks of summer and 28 weeks for the rest (52 weeks in a year). Not all the operational nodes are depicted in the tree in Figure 2 which is meant as an example. Similarly, only two operational scenarios for each strategic node are represented.

A time horizon of 10 years has been chosen according to the available dataset. This time horizon turned out to be suitable also to make observations in terms of battery replacement investments.

Given the parameters and variables listed in Table 1, 2 and 3, the stochastic multihorizon mathematical model for a charging site design and management follows. For a general introduction about Multihorizon Stochastic Optimisation and Programming theory see [21]. Note that the nomenclature is organised as follows: parameters will be identified by capital characters, while variables will be identified by non-capital characters. Indexes related to time periods, operational profiles, strategic nodes, scenarios, battery types and transformer types will always be placed at

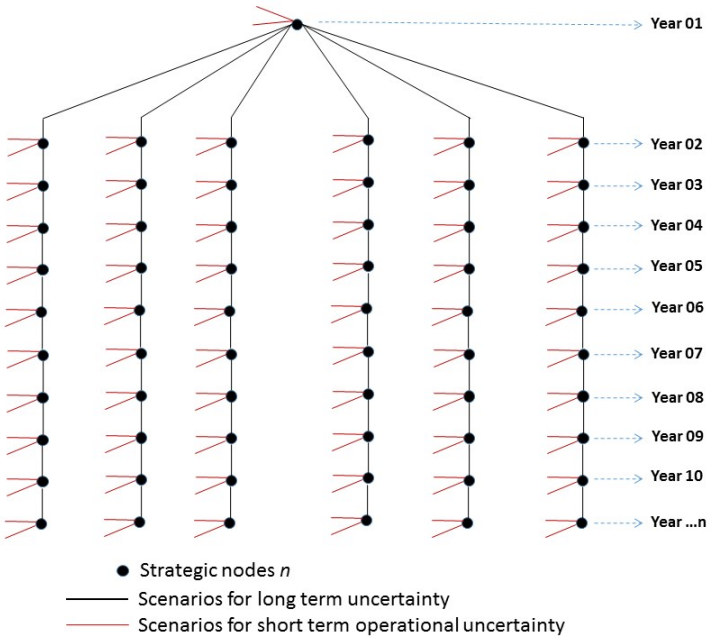

Figure 1: Stochastic multihorizon tree that summarises the model construction

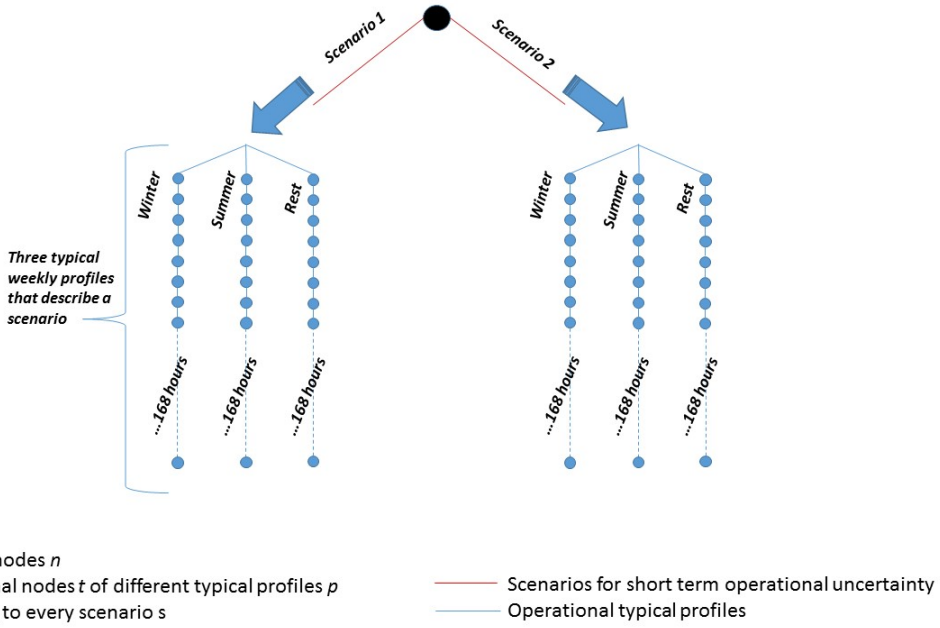

Figure 2: Details of short term scenarios. Every scenario is described by typical weekly profiles of winter, summer and the rest of the year. A hourly resolution is choosen.

the bottom of the main character. Abbreviations and words that better describe a parameter or a variable will be placed at the top of the main character.

4.2 Objective Function

$$MIN \sum_{n} P_n * \frac{1}{(1+r)^{Y_n}} * \Big(TC_n + TO_n \Big) \tag{1}$$

$$TC_n = R_n^{cost} * \lambda_n^R + \sum_j B_{n,j}^{cost} * \varepsilon_{n,j} + \sum_i T_{n,i}^{cost} * \theta_{n,i} + G^{cost} * g_n + G^{cab} * z * k \qquad \forall n \tag{2}$$

$$R_n^{cost} = R_n^L * R \qquad \forall n, p, s, t \tag{3}$$

$$B_{n,j}^{cost} = B_n^L * B_j \qquad \forall n, p, s, t \tag{4}$$

$$T_{n,i}^{cost} = T_n^L * T_i \qquad \forall n, p, s, t \tag{5}$$

$$TO_n = \sum_s P_s * \Bigg\{ \sum_p \omega_p * \Bigg(\sum_{t,i} P_{t,n,p,s} * f_{t,n,p,s,i}^{TD} + \sum_{t,i,j} P_{t,n,p,s} * f_{t,n,p,s,i,j}^{TB} \Bigg) \Bigg\} \qquad \forall n \tag{6}$$

$$P_{t,n,p,s} = P_n^L * P_{t,p,s}^{\beta} \qquad \forall n, p, s, t \tag{7}$$

The objective function minimises the net present value of operational costs TO_n and investment costs TC_n that will occur in every year represented by strategic nodes n. As different long term scenarios are considered (see the different branches of the tree in Figure 1), such actualised costs are multiplied by the related probability P_n.

As shown in equation 2 the total investment costs in every strategic node are related to renewable installation costs, battery installation costs, transformer upgrade costs and grid reinforcement costs. Equations 3, 4 and 5 define the investment costs of renewable plants, batteries and transformer in every strategic node n according to long term multipliers that forecast their future investment cost trend.

Operational costs are shown in equation 6 as the summation of $(P_{t,n,p,s} * f_{t,n,p,s,i}^{TD})$ that is the cost of the energy that flows from the transformer i to the load in every time step t embedded in every strategic node n, plus $(f_{t,n,p,s,i,j}^{TB} * P_{t,n,p,s})$ that is the cost of the energy that flows from the transformer i to the battery j in every time step t embedded in every strategic node n. As explained previously, we are sectioning the year into typical profiles p, therefore the operational costs have to be multiplied by the weight w_p that represents how many times a typical profile of

type p occurs in a year. As we are including also operational uncertainty, such energy flows have to be multiplied by P_s that represents the probability of every operational scenario s.

The electricity price $P_{t,n,p,s}$ is given by the forecast price $P^{\beta}_{t,p,s}$, multiplied by P^{L}_{n} that is a long term multiplier aiming at representing the price variation in the forthcoming years n.

4.3 Demand

$$f^{RD}_{t,n,p,s} * R^{eff} + \sum_{j} f^{BD}_{t,n,p,s,j} * B^{eff}_{j} + \sum_{i} f^{TD}_{t,n,p,s,i} * T^{eff}_{i} = D_{t,n,p,s} \qquad \forall n,p,s,t \tag{8}$$

$$D_{t,n,p,s} = D^{L}_{n} * D^{\beta}_{t,p,s} \qquad \forall n,p,s,t \tag{9}$$

Equation 8 assures that the demand is met by the energy flows from the transformer, from the renewable and from the battery.

The demand $D_{t,n,p,s}$ is given by the forecast demand $D^{\beta}_{t,p,s}$ multiplied by D^{L}_{n} that is a long term multiplier aiming at representing the demand variation in the forthcoming years n.

4.4 Renewable

$$q^{R}_{n} = \lambda^{R}_{n} \qquad \forall n | n = 1 \tag{10}$$

$$q^{R}_{n} = q^{R}_{n-1} + \lambda^{R}_{n} \qquad \forall n | n > 1 \tag{11}$$

$$q^{R}_{n} \leq R^{lim} \qquad \forall n \tag{12}$$

$$f^{RD}_{t,n,p,s} + \sum_{j} f^{RB}_{t,n,p,s,j} \leq q^{R}_{n} * R^{\beta}_{t,p,s} \qquad \forall n,p,s,t \tag{13}$$

The variable q^{R}_{n} keeps track of the renewable capacity available in every node n. In the first node, the available renewable capacity is equal to the number of units installed (equation 10) while in the following nodes it is equal to the capacity available in the previous node plus the additional units installed in the current node (equation 11). Space limitations might impose an upper bound in the maximum installable capacity (equation 12). The renewable operations in terms of flows to the load and to the battery are limited by the units installed multiplied by the forecast unitary production $R^{\beta}_{t,p,s}$ (equation 13).

4.5 Transformer

$$q^{T}_{n,i} = \theta_{n,i} * T^{cap}_{i} * F + \widehat{T}^{cap} * F \qquad \forall i,n | n = 1 \tag{14}$$

$$q^T_{n,i} = q^T_{n-1,i} + \theta_{n,i} * T^{cap}_i * F \qquad \forall i, n | n > 1 \tag{15}$$

$$\sum_j f^{TB}_{t,n,p,s,i,j} + f^{TD}_{t,n,p,s,i} \leq q^T_{n,i} \qquad \forall n, p, s, t, i \tag{16}$$

$$\sum_i q^T_{n,i} \leq D^{peak}_n * (1 + T^{\%}) \qquad \forall n \tag{17}$$

$$\sum_i q^T_{n,i} \leq T^{lim} \qquad \forall n \tag{18}$$

The variable $q^T_{n,i}$ keeps track of the transformer additional capacity available in every node n. In the first node the transformer upgrade is equal to the additional installed capacity, while in the following nodes it is equal to the capacity available in the previous nodes plus the additional installation in the current node (equations 14 and 15 respectively). Given that an existing transformer will have to be already available in the site, the flows out the transformer are limited by the available existing and new capacity in every node (equation 16). As explained in details in Section 3.2, the total transformer capacity in every node have to be limited to a certain percentage $T^{\%}$ of the peak demand. This will prevent the model from acting in a greedy way by hugely oversizing the transformer to face the increasing demand forecast in the following years. But still it will allow a slightly oversized installation to prevent overload issues. Therefore constraint 17 guarantees a technically feasible choice to prevent the negative implications of oversizing and overloading described in Section 3.2. Moreover, distribution transformer sizes are supposed to lie within certain dimensions that impose upper bounds T^{lim} in the maximum allowed typical size (constraint 18). Typical values for small, medium, large distribution transformers will be discussed in Section 5.5. According to the particular application and eventually rule and regulations of the particular country, different limitations may occur.

4.6 Grid Reinforcement

$$g_n = 0 \rightarrow c^{REF}_n = \widehat{T}^{cap} * F \qquad \forall n | n = 1 \tag{19}$$

$$g_n = 0 \rightarrow c^{REF}_n = c^{REF}_{n-1} \qquad \forall n | n > 1 \tag{20}$$

$$g_n = 1 \rightarrow c^{REF}_n = \sum_i q^T_{n,i} \qquad \forall n \tag{21}$$

$$\sum_i q^T_{n,i} > G^{\%} * \widehat{T}^{cap} * F \rightarrow g_n = 1 \qquad \forall n | n = 1 \tag{22}$$

$$\sum_i q^T_{n,i} > G^{\%} * c^{REF}_{n-1} \rightarrow g_n = 1 \qquad \forall n | n > 1 \tag{23}$$

$$\sum_j f^{TB}_{t,n,p,s,i,j} + f^{TD}_{t,n,p,s,i} \leq z * G^{cap} * H \qquad \forall n, p, s, i \tag{24}$$

As already outlined in Section 3, grid reinforcement costs will occur when the transformer has to be upgraded above a certain limit. In particular, it is assumed that grid reinforcements occur when the transformer capacity has to be upgraded of an amount that is greater than a certain percentage $G^{\%}$ of the current available capacity. In order to include this into the model, it is necessary to use a variable c^{REF}_n that keeps track of the transformer reference capacity in every strategic node. As long as the transformer is upgraded below a certain percentage of the current capacity, the reference variable c^{REF}_n will remain the same. When the transformer capacity will be upgraded above the limit, then the reference variable c^{REF}_n will be updated. This is achieved by the following set of constraints.

Constraints 19, 20 and 21 define what happens to the reference variable c^{REF}_n if grid reinforcements occur or not. If no grid reinforcements happen in the first strategic node, the reference variable c^{REF}_n is simply equal to the existing transformer capacity (constraint 19). If no grid reinforcements happen in any other strategic node, then the reference variable c^{REF}_n remains unchanged and equal to the value it had in the previous strategic node (constraint 20). If a grid reinforcement happens in any of the strategic nodes, then the reference variable c^{REF}_n is updated by adding the new capacity $q^T_{n,i}$ to the existing capacity (constraint 21).

Constraints 22 and 23 define in which circumstances grid reinforcements happen. In the first strategic node, if the upgraded transformer capacity is greater than a certain percentage $G^{\%}$ of the initial existing capacity, then a grid reinforcement occurs and the binary variable g_n has to be 1 (constraint 22). In every other strategic node, if the upgraded transformer capacity is greater than a certain percentage $G^{\%}$ of the reference capacity in the previous node c^{REF}_{n-1}, then a grid reinforcement occurs (constraint 23).

All the above statements can be written in a form suitable for optimisation models by using proper BigM formulations or by including indicator constraints. For further reading about handling indicator constraints in MIP problems see [50].

Finally constraint 24 ensures that the chosen cable capacity is suitable for the forecast energy flows that will be needed in every strategic node.

4.7 Battery Choice and Degradation

$$q^B_{n,j} = \varepsilon_{n,j} * B^{cap}_j \qquad \forall j, n | n = 1 \tag{25}$$

$$h_{n,j}^{INIT} = B_j^{thr} * \varepsilon_{n,j} \qquad \forall j, n | n = 1 \tag{26}$$

$$h_{n,j}^{FIN} = B_j^{thr} * \varepsilon_{n,j} - \sum_s P_s * \left(\sum_p \omega_p * \sum_t \frac{f_{t,n,p,s,j}^{BD}}{B_j^{eff}} \right) \qquad \forall j, n | n = 1 \tag{27}$$

$$h_{n,j}^{INIT} = h_{n-1,j}^{FIN} + B_j^{thr} * \varepsilon_{n,j} \qquad \forall j, n | n > 1 \tag{28}$$

$$\sum_j b_{n,j}^{REP} = 1 \rightarrow \sum_j h_{n-1,j}^{FIN} = 0 \qquad \forall n | n > 1 \tag{29}$$

$$b_{n,j}^{REP} = 1 \rightarrow q_{n,j}^{B} = \varepsilon_{n,j} * B_j^{cap} \qquad \forall j, n | n > 1 \tag{30}$$

$$h_{n,j}^{FIN} = h_{n-1,j}^{FIN} - \sum_s P_s * \left(\sum_p \omega_p * \sum_t \frac{f_{t,n,p,s,j}^{BD}}{B_j^{eff}} \right) + B_j^{thr} * \varepsilon_{n,j} - h_{n,j}^{REP} \qquad \forall j, n | n > 1 \tag{31}$$

$$b_{n,j}^{REP} = 0 \rightarrow q_{n,j}^{B} = q_{n-1,j}^{B} * \left(1 - \frac{h_{n-1,j}^{INIT} - h_{n,j}^{INIT}}{B_j^{thr}} * B_j^{fade}\right) \forall j, n | n > 1 \tag{32}$$

$$\sum_j \theta_{n,j} \leq 1 \qquad \forall n \tag{33}$$

$$\varepsilon_{n,j} \neq 0 \rightarrow \theta_{n,j} = 1 \qquad \forall n \tag{34}$$

For the battery choice we refer to the real world situation in which different standard types of batteries are available in the market with certain properties (price, capacity, efficiency, rating, etc). Hence the model chooses one type of battery j with a certain capacity B_j^{cap} and then the optimal number of units of that type to be installed $\varepsilon_{n,j}$ in order to create the battery bank.

The variable q_n^B keeps track of the total storage capacity available in every node n. The storage capacity available in the first year is equal to the capacity of the battery of type j multiplied by the number of units to be installed (constraint 25).

Two main degradation issues are taken into account in the model: lifetime throughput and capacity fade.

The model keeps track of the residual lifetime throughput in every strategic node through the variables $h_{n,j}^{INIT}$ and $h_{n,j}^{FIN}$ that define the lifetime throughput at the beginning of every year and at the end of every year respectively. On the first node the initial lifetime throughput is given by the throughput of the chosen battery multiplied by the number of units installed (constraint 26); while the final throughput is given by the initial value minus the total energy that has been drawn in the different typical periods and for the different operational scenarios (constraint 27).

In all the other nodes the lifetime throughput at the beginning of the year, is equal to the residual throughput at the end of the previous year, plus the additional throughput derived from new additional battery installation (constraint 28).

However, as discussed in Section 3, when adding new batteries, the whole battery bank has to be replaced as it is not recommended to keep batteries of different age and type working together. Hence when a battery replacement occurs in a strategic node ($b_{n,j}^{REP} = 1$), the lifetime throughput has to be zero at the end of the previous year (constraint 29) and the battery installation is simply equal to the new installation that occurs in the node (constraint 30).

Constraint 29 is very strong as it imposes a strict value of lifetime throughput at the end of a year if a replacement occurs the year after. It is reasonable to let the model free to decide if it is worthy to replace a battery whatever its residual throughput is. In fact in a multihorizon framework, a decreasing trend of battery costs together with an increasing trend of demand, may bring to decisions in which it is worthy to replace a small battery bank with a larger one in a certain year, instead of carrying on using the residual throughput of the existing bank from the previous year (that may be insufficient to fulfill the increased demand requirements of the forthcoming years). Hence, in order to give the model freedom in deciding if it is worthy to replace a battery bank that still has a residual throughput, a variable $h_{n,j}^{REP}$ is inserted in constraint 31. In particular, the residual throughput at the end of every strategic node (excluded the first one) is given by the residual throughput at the end of the previous node, minus the total energy that has been withdrawn from the battery in the operations of the current node, plus the additional throughput of the new battery bank that is eventually installed, minus the variable $h_{n,j}^{REP}$. What happens in such constraint is that if the term $\varepsilon_{n,j}$ is greater than zero, a replacement occurs therefore the residual throughput of the previous year has to be zero (constraints 29 and 30) but the variable $h_{n,j}^{REP}$ can get a value greater than zero that is the residual throughput that may still be there when doing such battery replacement. This way, whatever the residual throughput is, a battery replacement can occur if certain combinations of forecast demand increment and cost reductions arise.

Constraint 32 aims at including the capacity fade that occurs in the battery as a further degradation term in addition to the throughput discussed above. In particular, if no replacement occurs, the battery capacity will not remain the same, but it will decrease as a function of the used throughput. As discussed in Section 3, as long as the battery usage is kept within the throughput, the manufacturers guarantee that the capacity will not drop below a certain limit B_j^{fade}. Therefore it is possible to approximately quantify the capacity fade $\%fade$ at the end of every year through a simple proportion $[B_j^{thr} : B_j^{fade} = (h_{n-1,j}^{INIT} - h_{n,j}^{INIT}) : \%fade]$ that gives us informations about the percentage of capacity fade associated with a certain usage of throughput. This is inserted in constraint 32 to properly keep track of the available storage capacity and penalise it according to

capacity fade issues.

Constraint 33 limits the choice of battery units to a one single type, so that batteries of the same type will be installed in the battery bank.

Finally constraint 34 links the two decisional variables $\varepsilon_{n,j}$ and $\theta_{n,j}$.

Constraints 29, 30 and 32 can be expressed using BigM formulations or indicator constraints. It is important to note that in this case the use of the BigM formulation is imposing an upper bound on the maximum installable capacity and on the maximum throughput, hence unless there are clear informations about maximum installable storage capacity (in terms of space, or weight for instance) the use of indicator constraints could be more appropriate in this case. For further reading about handling indicator constraints in MIP problems see [50].

4.8 Battery Operations

$$b^{SOC}_{t,n,p,s,j} = B^{init}_j * q^B_n \qquad \forall n,p,s,t,j|t=0 \tag{35}$$

$$b^{SOC}_{t,n,p,s,j} = B^{fin}_j * q^B_n \qquad \forall n,p,s,t,j|t=T \tag{36}$$

$$b^{SOC}_{t,n,p,s,j} = b^{SOC}_{t-1,n,p,s,j} - f^{BD}_{t,n,p,s,j} * \frac{1}{B^{eff}_j} + \sum_i f^{TB}_{t,n,p,s,i,j} * T^{eff}_i + f^{RB}_{t,n,p,s,j} * R^{eff}_w \qquad \forall n,p,s,t,j|t>0 \tag{37}$$

$$\sum_i f^{TB}_{t,n,p,s,i,j} + f^{RB}_{t,n,p,s,j} \leq y_{t,n,p,s,j} * BigM \qquad \forall n,p,s,t,j \tag{38}$$

$$f^{BD}_{t,n,p,s,j} \leq (1 - y_{t,n,p,s,j}) * BigM \qquad \forall n,p,s,t,j \tag{39}$$

$$b^{SOC}_{t,n,p,s,j} \leq q^B_n \qquad \forall n,p,s,t,j \tag{40}$$

$$b^{SOC}_{t,n,p,s,j} \geq B^{ch}_j * q^B_n \qquad \forall n,p,s,t,j \tag{41}$$

$$f^{BD}_{t,n,p,s,j} * \frac{1}{B^{eff}_j} \leq B^{rt}_j * q^B_n \qquad \forall n,p,s,t,j \tag{42}$$

$$\sum_i f^{TB}_{t,n,p,s,i,j} * T^{eff}_i + f^{RB}_{t,n,p,s,j} * R^{eff} \leq B^{rt}_j * q^B_n \qquad \forall n,p,s,t,j \tag{43}$$

The variable q^B_n keeps track of the storage capacity available in every node n.

Constraints 35 and 36 define the battery state of charge at the beginning and at the end of every typical profile respectively.

Equation 37 defines the battery state of charge in every time step as the difference between the state of charge in the previous time step minus the energy drawn and plus the energy that flows inside. Flows in and out the battery are mutually exclusive as imposed by constraints 38 and 39.

The battery maximum capacity and minimum state of charge to avoid permanent damage are defined in constraints 40 and 41.

The battery rating is defined in constraints 42 and 43 where flows in and out are limited by the C-rating properties of the particular battery.

5 Real World Data Collection

5.1 Battery Data

Current battery prices, throughput values and lifetime properties can be found in [51] where different data for various batteries from different manufacturers are proposed. According to this source, the battery cost per kWh is currently set in a range around 800 - 1000 $/kWh for a kWh throughput per kWh capacity in a range around 2000 - 3000 kWh. This is in line also with what is discussed in [52] and [53]. According to [51], higher throughput properties in the range of 7000 - 10000 kWh throughput per kWh capacity have a cost that is set around 2000 - 2500 $/kWh.

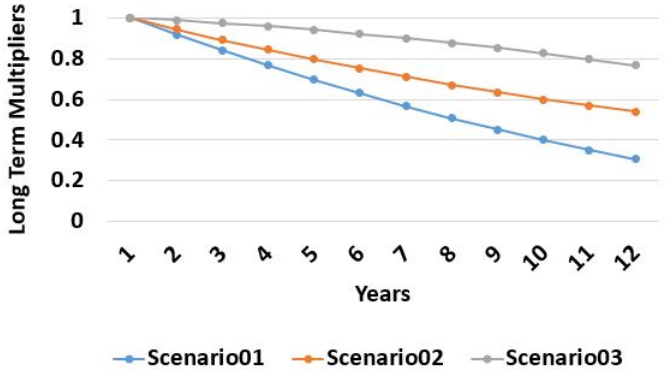

Figure 3: Long term multipliers to calculate battery projected costs in the forthcoming years

Future battery cost projections are discussed in [54] where different forecast trend proposed by BNEF, NAVIGANT and EIA are shown as well as an averaged curve. Long term multipliers that trace such forecast are shown in Figure 3 and used in the mathematical model to define the battery prices in different strategic nodes. Scenario01 is tracing BNEF optimistic prediction, Scenario03 is tracing EIA pessimistic prediction while Scenario02 is tracing the averaged curve. NAVIGANT prediction is not shown as it was overlapping with BNEF optimistic prediction.

For further readings about battery cost projections see [55] and [56].

5.2 Renewable Data

Current and projected future costs for photovoltaic plants are discussed in [57], [58] and [59]. The former in particular analyse different scenarios from which suitable long term multipliers can be derived as shown in Figure 4. According to the mentioned sources, the current average cost of a photovoltaic plant (solar panel and installation) is set around 700 $/kW.

The unitary production of a photovoltaic plant can be found in the PVWatts calculator available online through the NREL website [60]. Figure 5 shows the photovoltaic production for typical weeks in Norway.

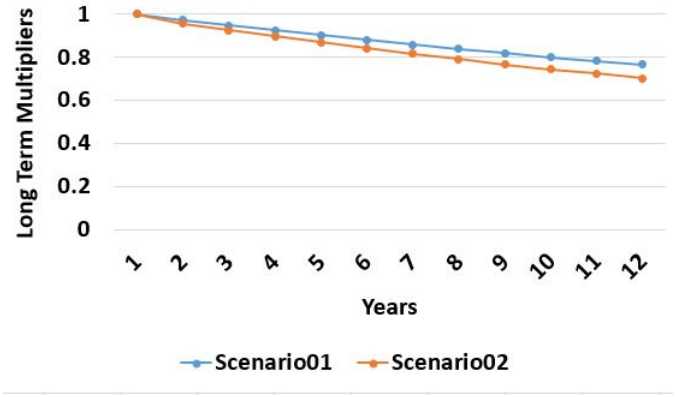

Figure 4: Long term multipliers to calculate photovoltaic projected costs in the forthcoming years

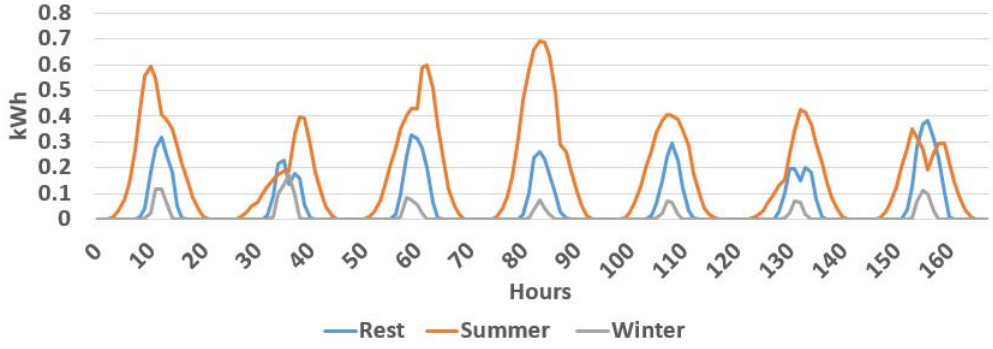

Figure 5: Example of renewable production for one kW photovoltaic panel, throughout typical weeks of summer, winter and the rest of the year. Different samples have been used in every strategic node to allow a better representation of uncertainty

5.3 Electricity Price Data

Both current and historical electricity price values are available from the Nord Pool website [61]. Figure 6 shows the price trend for typical weeks in Norway.

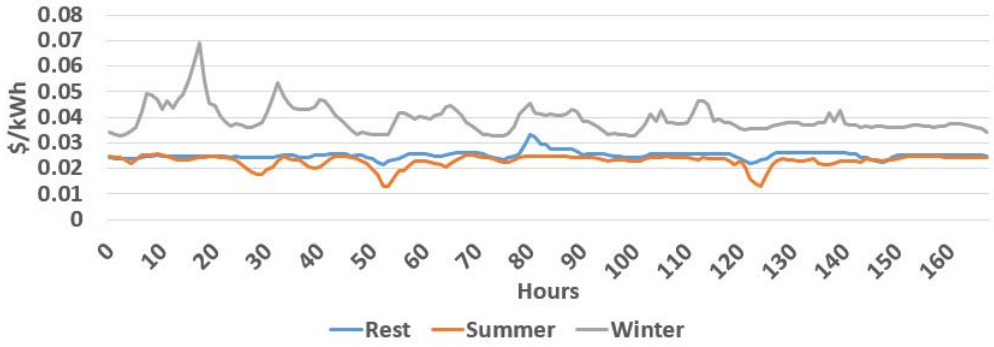

Figure 6: Example of electricity price in Norway, throughout typical weeks of summer, winter and the rest of the year. Different samples have been used in every strategic node to allow a better representation of uncertainty

Long term projection of electricity price in Norway has been discussed in [62], [63] and [64]. The former in particular shows three different scenarios for price forecasts. According to such study, long term price multipliers are shown in Figure 7.

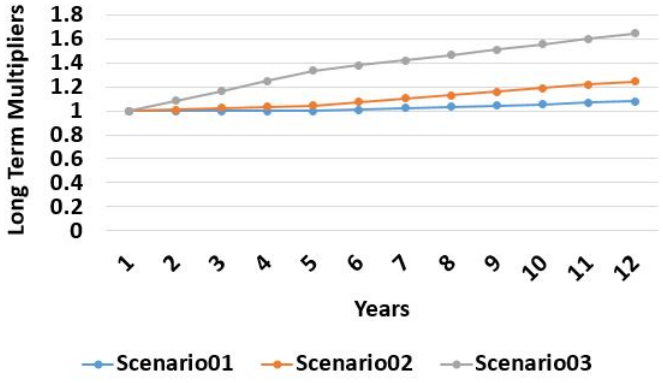

Figure 7: Long term multipliers to calculate the projected electricity price in the forthcoming years

For an overview of electricity price projection in Europe it is possible to refer to [65].

5.4 Demand Data

Hourly demand data for a whole year have been collected from a real charging site, Ladetorget in Moss, Norway. Figure 9 shows the demand trend for typical weeks in different seasons.

As for long term demand development, the basic assumption is that the power needed will approximately double every second year, mainly due to charging at higher power levels, but also due to further increasing penetration of electric vehicles in the norwegian transportation market.

Demand hourly data and future projection have been provided by eSmartSystems, energy company in Halden, Norway. Further readings about electric vehicles demand development in Norway can be found in [66]. While for an overview related to electric vehicles demand development in Europe see [67] and [68].

Figure 8 shows the long term demand multipliers that describe two scenarios of future demand development. In particular, Scenario01 is optimistic and assumes that demand will double every second year as mentioned above. While Scenario02 is a pessimistic one, that mitigates the effect of Scenario01, assuming that the demand will keep on increasing for a limited period and then settle. This is made to take into account that in Norway, electric vehicles have seen a very high diffusion mainly due to strong government incentives (i.e. electric vehicles are exempt road tax, public parking fees, toll payment as well as being able to use bus lanes). But these incentives are in effect until 2018 as further discussed in [69]. Hence how this disappearance of incentives will affect the market is unknown, but needs to be taken into account in future scenarios generation.

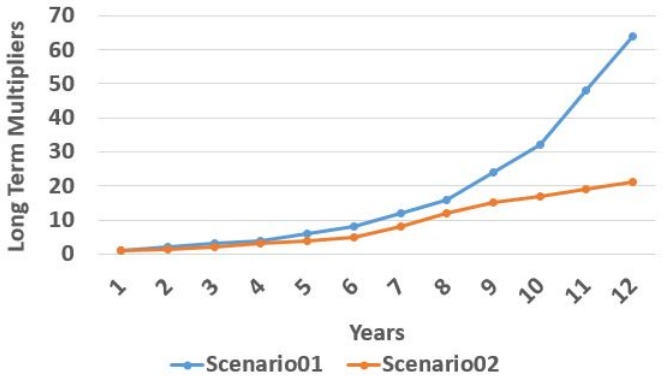

Figure 8: Long term multipliers to calculate the projected demand in the forthcoming years

5.5 Transformer Data

For this work and for the particular case of a charging site we are interested in distribution transformers size and costs. The ABB webiste [70] proposes three typical ranges for distribution transformers according to the particular application involved. Small distribution transformers (0 - 315 kVA) are suitable for residential distribution loads, as well as light commercial or industrial loads. Medium distribution transformers (316 - 2499 kVA) are used to step down high voltage to low voltage for energy distribution, mainly in the countryside or low-density populated areas. Large

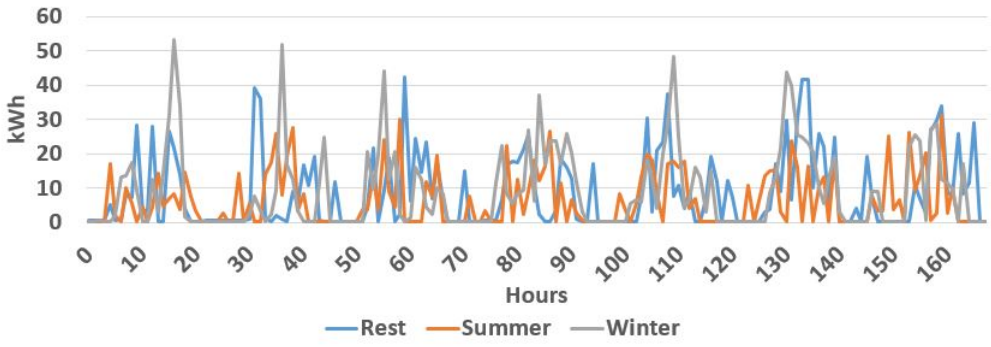

Figure 9: Example of demand trend for a charging site throughout typical weeks of summer, winter and the rest of the year. Different samples have been used in every strategic node to allow a better representation of uncertainty

distribution transformers (2500 - 10000 kVA) are used for receiving energy from higher voltage levels and to transform and distribute this energy to lower voltage substations or directly to large industrial consumers.

This gives a broad indication of the available range and dimensions and puts an upper bound on the maximum size allowed for typical real world applications. Depending on the particular site and eventually on rule and regulations of a particular country, the upper limit in the transformer size can actually fall within one of the three above mentioned typical ranges. Sensitivity analyses assuming different upper bounds can be performed to evaluate the different response and choice of the proposed optimisation model.

Different typical transformer sizes and related investment costs updated in 2016 can be found in [71] and are summarised in Table 4. According to the proposed numbers, it is reasonable to assume an approximated average unitary cost equal to 15 $/kVA that can be suitable for linear programming models.

The lifetime of a transformer can be realistically assumed around 20 years more or less [48].

We do not assume long term uncertainty in the transformer price because this is a very established technology that haven't changed very much for the last years.

5.6 Grid Reinforcement Data

For grid reinforcement it is possible to consider a cable cost per km assuming that new cables installation will be needed when increasing the size of an existing transformer above a certain limit that exceeds the available capacity of the existing cables. Grid reinforcement costs can be found in the Sinterf Planbok [72] and are higher for installations inside the city compared to installations outside the city. In particular, the digging part for cable installation which is around 75000 $/km

Table 4: Transformer costs

Capacity (kVA)	Price ($)
25	1235
50	1706
75	2106
100	2435
160	3233
200	3822
250	4156
315	4896
400	5885
500	6851
630	8363
800	9909
1000	11597
1250	13966
1600	17339
2000	20776

inside the city and 33000 $/km outside the city. As for the cost of cables, this varies with both the capacity and the length of the cable. A unitary cost can be defined according to data provided in [73] and summarised in Table 5.

Table 5: Cable costs

Size (kcmil)	Ampacity (Amps)	Price ($/km)
500	332	39360
750	405	85280
1000	462	123640

This gives a broad idea of the grid reinforcement costs. As the lifetime of cables is very long, it is reasonable to assume that within a time horizon of 10 years, if such an investment is needed, it will be done once and cables will be oversized according to the load forecast. It is straightforward that the trade off between proper battery installation and proper cable oversizing according to the related expenses and load forecast is worthy to be investigated through the proposed optimisation model.

As a general guideline, a transformer should be placed near the load, as minimizing the distance between the unit and the main load results in minimizing energy loss and voltage reduction [48]. Hence in urban areas, as a general guideline, the load points (such as a charging station) should lie within a range of 3-5 km more or less from the transformer. Of course, there can exist situations in which distance is higher especially in rural areas where the range can be much larger.

It is important to note that it is not the charging station operator (owner) that fully invest to cover such costs. This is done mainly by the DSO, but the charging station operator has to pay

anyway a fee to the DSO which partly covers the DSOs costs. Moreover, grid reinforcement costs can include a wider variety of other costs related to electrical components, substation upgrade procedures, additional connections etc. Hence the cable cost per km provided above, can be considered as a representative cost aimed at defining a reasonable starting point for further sensitivity analyses. In particular, sensitivity analyses assuming different grid reinforcement costs according to different distances from transformer and load can be performed to evaluate the different response and choice of the proposed optimisation model.

5.7 Scenarios Selection

The six selected scenarios for testing are shown in Figure 10 and aim at capturing different combinations of battery and renewable costs long term variations, as well as demand and electricity price long term development.

6 Computational Experiments

The main research question investigated in the computational experiments, is related to an important trade-off that has to be addressed in the proposed decision problem: given that the investment costs of battery storage and renewable resources will drop in the forthcoming years, how should grid reinforcement be timed in terms of transformers and cables? Cables represent one of the highest cost components when upgrading such systems, and costs increase with the cable size and length. Therefore, given a forecast for demand increment, we are interested in analysing whether battery and renewable investment spread out over the years, can mitigate - or even make us able to avoid - the costs of grid reinforcements needed today. Moreover, even if batteries and renewable might still be too expensive today, their costs may drop through the years making them more convenient in the future. This may allow savings today in terms of grid reinforcements because smaller installations can be done recognizing that future demand increment will then be covered by additional storage and renewable technologies whose costs are supposed to become cheaper.

The computational tests illustrates how different conditions affect the investment decisions. In particular, the analysis shows the effect of the distance between charging sites and transformers for the trade-off between grid reinforcement, batteries and renewable investments; the influence of the demand forecast on the worthiness of batteries and renewable; the influence of battery performance and related costs. We will finally discuss the value of a multihorizon perspective versus traditional approaches in light of the proposed tests.

For testing purposes we assume an existing site that is undersized compared to the forecast increment in demand, and where an upgrade decision has to be taken already in the first year. That might include an upgrade of the transformer, the installation of new cables, the installation

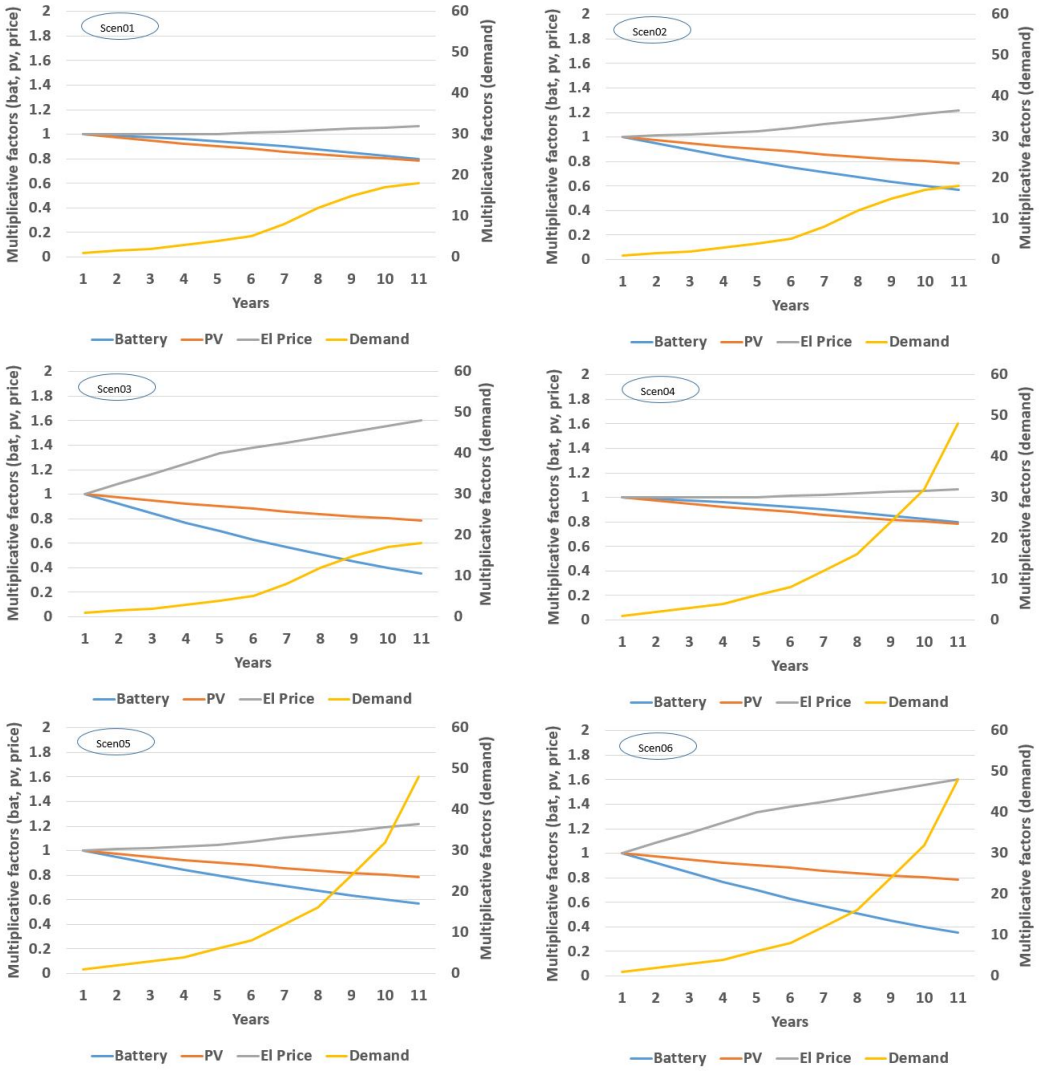

Figure 10: Long term scenarios used in the model computational testing

of batteries or renewables. The decision can be any combination of these. The decision taken in the first year includes the knowledge that further installations can be made in every year following as well, but then with more information.

6.1 Effect of Charging Site Location and Distance from Transformer Substation

The tests includes sensitivity analyses to understand how the cost of cables linked to the distance between charging site and transformer substation can affect the investment decisions. As seen in the data section, the cable costs represent a high component of the site upgrade costs. This is influenced not only by the size of cables (that is linked to the upstream transformer size), but also by the length (that is linked to the distance between the transformer substation to the charging site itself). Hence, closer substations will be cheaper than those which are far away. The following tables show how does this affect investment decisions in different energy units.

The tables show decisions taken in every year belonging to all the scenarios shown in Figure 10. Columns *Bat* shows the investments in battery capacity, columns *Ren* shows the investments in renewable photovoltaic plants, while the column *Reinf* shows the investment decisions in terms of grid reinforcement (this indicates the maximum power in watts which the new upgraded cables are able to carry. Transformer is upgraded accordingly).

When the distance from the charging site to the transformer increases, the investments in grid reinforcement on the first year become lower resulting in higher and earlier investments on batteries in the following years. Note that, even with very high grid reinforcement costs (Table 9), with the given scenarios the batteries are still too expensive to be installed in the first year and large battery installations happen anyway around the 7th and 8th year when prices are likely to be more or less 80% of the current price.

In tables 8 and 9 results indicate that very small battery installations are done the year before a larger installation. In such cases the battery is small and quicly degraded in terms of throughput in order to allow a larger installation the year after at a better price.

In scenario 6 of tables 7, 8 and 9 note that a large battery installation is proposed in the 9th year. This is due to the particular scenario structure that is visible in Figure 10 where the stronger battery price decrement is combined with a strong demand increment. Hence to take advantage of the price reduction in batteries in combination with a demand increment that can allow a high investment, the model is postponing the large battery installation to the 9th year, but still installing a battery on the 7th year. This does not happen in scenario 3 because even if the battery learning curve is the same, the demand increment is smoother and does not justify larger investments in batteries.

In these tests it is clear that the demand curve is affecting the battery installation in terms

of both timing and sizing. Battery installation is slightly later for scenarios 1, 2 and 3 where the demand curve is growing less, compared to scenarios 4, 5 and 6 where the demand curve is increasing rapidly and strongly throughout the whole time horizon. Similarly battery installation in terms of capacity is lower for scenarios 1, 2 and 3 where the demand increment is lower, and it is much higher in scenarios 3, 4 and 5 where the demand increment is stronger. It is important to note that the grid reinforcement made on the root node (year 1) will have to cover all the 6 future scenarios and in particular both demand curves, the highest one and the lower one. In order to properly cover the highest demand curve of scenarios 4, 5 and 6, cables will result in being slightly oversized for the lower demand curve of scenarios 1, 2 and 3 (that means, if only scenarios 1, 2 and 3 were available, the model would have installed smaller cables). This explains why the battery installation for scenarios 1, 2 and 3 happens later: in fact, in such scenarios the demand is increasing less but cables installation on the first year is sized to cover also a higher demand curve, hence for scenarios 1, 2 and 3 it is possible to exploit cables more and postpone battery installation. The high demand scenario strongly affects decisions in the first year and thereby also affects how the other scenarios with lower demand curves are managed.

Finally, the renewable photovoltaic resource is installed very late, probably due to the fact that in this particular application with data from Norway, a good portion of the year is characterized by a very low solar production due to the long winter season.

The forthcoming tests show how the demand curve can strongly influence the battery and renewable investment decision.

Table 6: Results: 1km distance from site to transformer substation

Year	Bat (kWh)	Reinf (kW)
1		643

	Scenarios											
	01		02		03		04		05		06	
Year	Bat (kWh)	Ren (kW)	Bat (kWh)	Ren (kW)	Bat (kWh)	Ren (kW)	Bat (kWh)	Ren (kW)	Bat (kWh)	Ren (kW)	Bat (kWh)	Ren (kW)
2												
3												
4												
5												
6												
7												
8	951		951		951		3438		3438		3438	
9												
10												

Table 7: Results: 2km distance from site to transformer substation

Year	Bat (kWh)	Reinf (kW)
1		450

	Scenarios											
	01		02		03		04		05		06	
Year	Bat (kWh)	Ren (kW)	Bat (kWh)	Ren (kW)	Bat (kWh)	Ren (kW)	Bat (kWh)	Ren (kW)	Bat (kWh)	Ren (kW)	Bat (kWh)	Ren (kW)
2												
3												
4												
5												
6												
7							5265		5265		1327	
8	1493		1493		1493							
9											5265	
10								307		307		307

Table 8: Results: 3km distance from site to transformer substation.

Year	Bat (kWh)	Reinf (kW)
1		430

	Scenarios											
	01		02		03		04		05		06	
Year	Bat (kWh)	Ren (kW)	Bat (kWh)	Ren (kW)	Bat (kWh)	Ren (kW)	Bat (kWh)	Ren (kW)	Bat (kWh)	Ren (kW)	Bat (kWh)	Ren (kW)
2												
3												
4												
5												
6							59		59		59	
7	59		59		59		5518		5518		1386	
8	1552		1552		1552							
9											5518	
10								354		354		354

Table 9: Results: 4 to 10 km distance from site to transformer substation.

Year	Bat (kWh)	Reinf (kW)
1		411

	Scenarios											
	01		02		03		04		05		06	
Year	Bat (kWh)	Ren (kW)	Bat (kWh)	Ren (kW)	Bat (kWh)	Ren (kW)	Bat (kWh)	Ren (kW)	Bat (kWh)	Ren (kW)	Bat (kWh)	Ren (kW)
2												
3												
4												
5												
6							110		110		110	
7	110		110		110		5757		5757		1437	
8	1603		1603		1603							
9											5757	
10								570		570		570

6.2 Influence of Demand Forecast on the Worthiness of Batteries and Renewable

From the previous tests it was clear how the demand forecast trend can strongly affect decisions in terms of battery installation.

In this section we will investigate deeper the demand forecast influence on the battery and renewable investment decisions. For that purpose we run sensitivity analyses by considering how different demand curves would affect the model decisions.

Figure 11 summarises tests made by considering a charging site that is 1 km distant from the transformer substation. Different demand curves are shown and, for every curve, a dot point indicates on which year a battery installation happens with the related installed capacity. Moreover, the related cables upgrade on the first year is indicated in the legend for every curve. Note that the legend indicates for every series, the maximum power in kW which the new upgraded cables are able to carry (the transformer is upgraded consequently).

Note that the higher the demand increment is, the later the battery installation occurs and the greater the battery capacity installed is. This is due to the fact that, higher demand increment means higher battery capacity needed and therefore higher investment. The higher the battery capacity, the later the investment in order to take advantage of the battery price forecast dropping. Hence the ability to look ahead in battery prices combined with the ability to properly forecast the demand trend, is crucial to make optimal choices in terms of cable size today and future battery installations. For this particular set of tests, no renewable has never been chosen within the optimal solution.

Figures 12 and 13 show the results for a set of tests made by considering a charging site that is

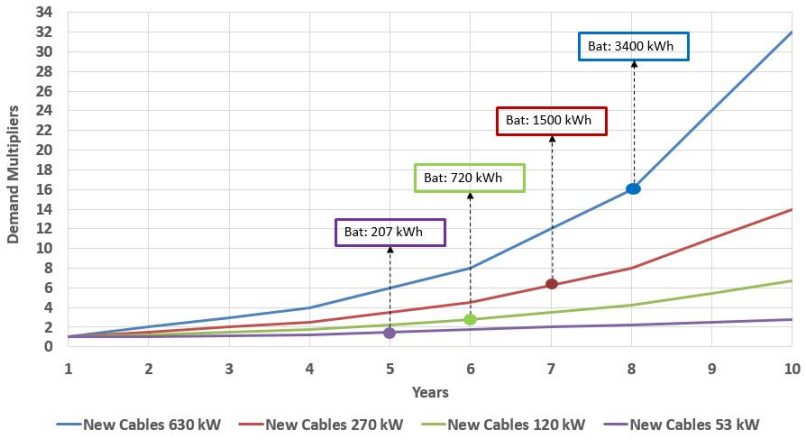

Figure 11: Battery installation and grid reinforcement decisions for different demand forecast trends considering a 1 km distance from the charging site to the transformer substation.

5 km away from the transformer substation. Hence, a case study in which grid reinforcement costs are much higher compared to the previous one due to the longer distances involved. Compared to the previous set of tests, Figure 12 shows not only higher and earlier investments in batteries but also battery bank replacements for the lowest demand curves (violet and green). Still the main trend of postponing battery installation for higher demand increment is kept.

Moreover in this case study renewable installations are shown in Figure 13. Due to the high costs of grid reinforcement, the cable size is lower compared to the previous case study, and renewable generation is chosen in addition to batteries to meet the higher demand in the later years.

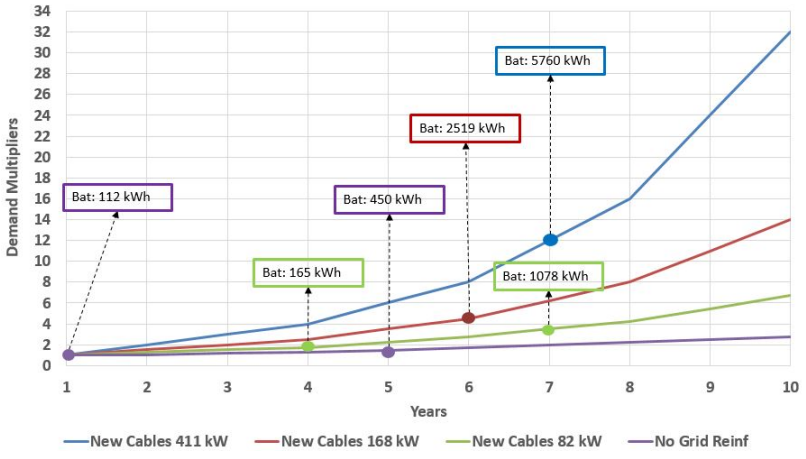

Figure 12: Battery installation and grid reinforcement decisions for different demand forecast trends considering a 5 km distance from the charging site to the transformer substation.

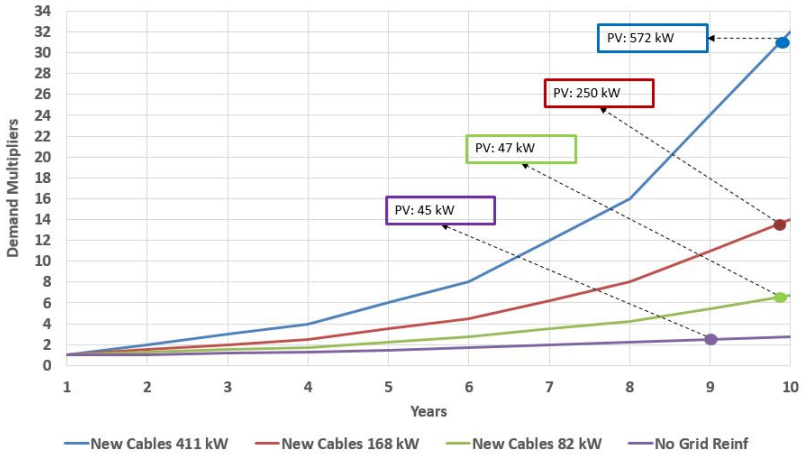

Figure 13: Photovoltaic installation and grid reinforcement decisions for different demand forecast trends considering a 5 km distance from the charging site to the transformer substation.

6.3 Influence of Battery Perfomance and Related Costs

In this set of tests we analyse the influence of battery performance and related costs on the optimal decisions. In particular, we run the model by considering a charging site that is 5 km distant from the transformer substation and we include the lower demand curve (violet one) from the previous tests. We observed previously that two battery installations occurred throughout the time horizon for this particular case study (see Figure 12 where battery is installed on the first year and then replaced on the 5th year for the lower demand curve in violet). Therefore we are now interested in looking deeper into this case study by providing the model with the choice between two batteries with different performances in terms of rating and efficiency. In particular, the model will choose between a battery of type 01 with better performane (0.8 efficiency and 0.5 rating), and a battery of type 02 with worse performance (0.7 efficiency and 0.25 rating). The cost of the battery 02 is assumed 800 $/kWh that is around the cheaper price that can be currently found in the market. Compared to battery 02, the cost of battery 01 is varied from slightly less than double, slightly more than double and three times larger in order to compare results. The objective is to give the reader an overview of how the costs and battery performance affects the model decisions and replacements decisions.

Figure 14 shows a case study where the cost of battery of type 01 with a better performance is almost double the cost of the battery of type 02 with lower performance. In this case the optimal choice is to always install the better battery of type 01 both in the first year and in the fifth year.

Figure 15 shows a case study where the cost of battery of type 01 with a better performance is now slightly higher than double compared to the battery of type 02. In this case the optimal choice is the best battery of type 01 in the first year, that will be replaced by the lower performing

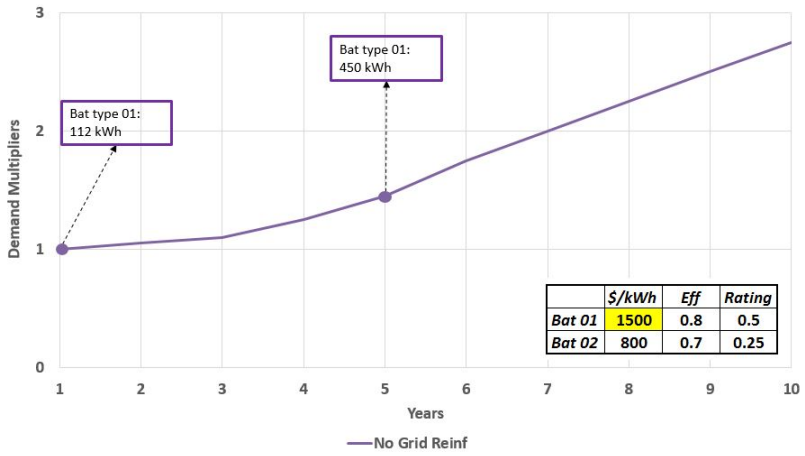

Figure 14: Installation decisions with choice between two batteries with different performances in terms of efficiency and rating. Case when the cost of a battery with better performance is assumed less than double compared to a battery type with lower performance

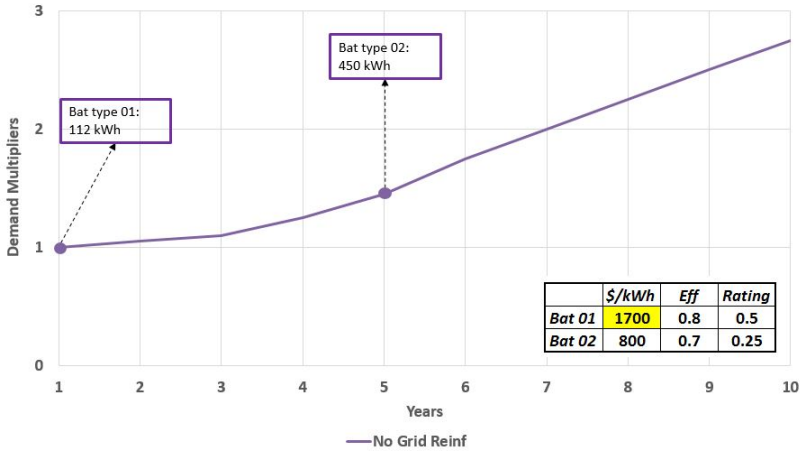

Figure 15: Installation decisions with choice between two batteries with different performances in terms of efficiency and rating. Case when the cost of a battery with better performance is assumed more than double compared to a battery type with lower performance, but still not too much higher

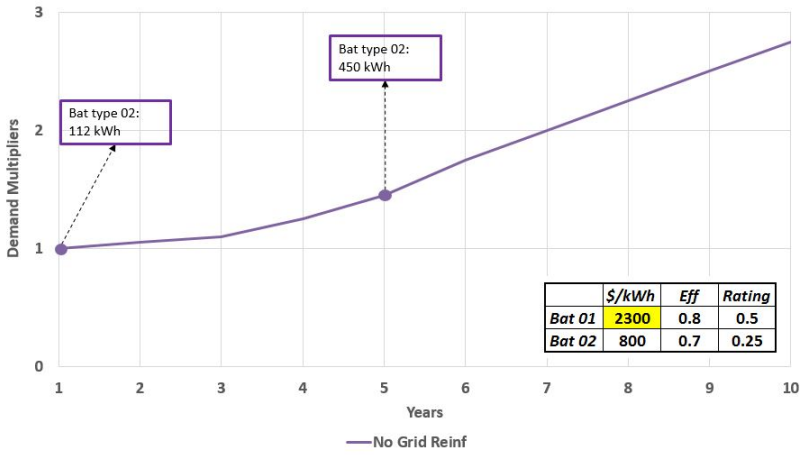

Figure 16: Installation decisions with choice between two batteries with different performances in terms of efficiency and rating. Case when the cost of a battery with better performance is assumed three times more compared to a battery type with lower performance

battery of type 02 in the fifth year. This is happening because the battery price will increase with the capacity. Given the low installation required in the first year, the cost of battery 01 is still more than compensated by the better efficiency and rating. But in the fifth year, higher capacity is required and the better performance is no longer worthy the higher costs. Therefore investment in a cheaper unit is preferred.

Figure 16 shows a case study where the cost of battery of type 01 with a better performance is assumed three times larger compared to the lower performing battery of type 02, hence a better battery performance is now very expensive. In this case the optimal choice is to go for the cheaper battery type both in the first year and in the fifth year when the bank is replaced. This is because the performance improvement in terms of efficiency and rating can not defend the higher cost.

Hence, the previous examples showed how sensible such decisions can be and how important it is to have a proper tool to support investment decisions in this field. Analyse the trade-off between cheaper batteries and more expensive batteries and their cost difference in the market can be crucial for industries involved in expansion decisions like the proposed one.

7 Conclusions

A mathematical model for the optimal design, extension and management of electric vehicles charging sites has been presented. It uses a multihorizon approach which compared to traditional approaches, allows to include both long-term uncertainty and short-term uncertainty in the model without an explosion of the scenario tree size as a consequence. The long-term uncertainty is im-

portant to be able to model the uncertain long-term trends, allowing the model to delay decisions until more information is known. The short-term uncertainty is important to estimate the consequence of investments in terms of capacity utilization of equipment under different operational settings.

The paper provides a complete real world dataset which can be of interest for similar studies. Extensive computational experiments and sensitivity analyses have been presented to gain insight in the factors driving the decisions under different assumptions. The analysis shows that both the long-term uncertainty and the short-term uncertainty play a major role in both timing, technology choice, and capacity decisions. Compared to traditional decision support approaches the model is able to take more precise decisions due to its multihorizon approach, the inclusion of battery degradation and the inclusion of grid rules and regulations limits that affect the final results.

Acknowledgments

The authors would like to acknowledge Sintef Energy Research for the precious help in providing costs of grid reinforcements for charging sites. Authors acknowledge also eSmart Systems for providing the demand data from a real charging site in Moss, Norway.

References

[1] Zhile Yang, Kang Li, and Aoife Foley. Computational scheduling methods for integrating plug-in electric vehicles with power systems: A review. *Renewable and Sustainable Energy Reviews*, 51:396–416, 2015.

[2] Junjie Hu, Hugo Morais, Tiago Sousa, and Morten Lind. Electric vehicle fleet management in smart grids: A review of services, optimization and control aspects. *Renewable and Sustainable Energy Reviews*, 56:1207–1226, 2016.

[3] Trine Krogh Kristoffersen, Karsten Capion, and Peter Meibom. Optimal charging of electric drive vehicles in a market environment. *Applied Energy*, 88(5):1940–1948, 2011.

[4] Yugong Luo, Tao Zhu, Shuang Wan, Shuwei Zhang, and Keqiang Li. Optimal charging scheduling for large-scale ev (electric vehicle) deployment based on the interaction of the smart-grid and intelligent-transport systems. *Energy*, 97:359–368, 2016.

[5] Mushfiqur R Sarker, Hrvoje Pandžić, and Miguel A Ortega-Vazquez. Optimal operation and services scheduling for an electric vehicle battery swapping station. *IEEE transactions on power systems*, 30(2):901–910, 2015.

[6] IJ Fernández, CF Calvillo, A Sánchez-Miralles, and J Boal. Capacity fade and aging models for electric batteries and optimal charging strategy for electric vehicles. *Energy*, 60:35–43, 2013.

[7] Abdorreza Rabiee, Mohammad Sadeghi, Jamshid Aghaeic, and Alireza Heidari. Optimal operation of microgrids through simultaneous scheduling of electrical vehicles and responsive loads considering wind and pv units uncertainties. *Renewable and Sustainable Energy Reviews*, 57:721–739, 2016.

[8] Yi Guo, Jingwei Xiong, Shengyao Xu, and Wencong Su. Two-stage economic operation of microgrid-like electric vehicle parking deck. *IEEE Transactions on Smart Grid*, 7(3):1703–1712, 2016.

[9] Shengyin Li, Yongxi Huang, and Scott J Mason. A multi-period optimization model for the deployment of public electric vehicle charging stations on network. *Transportation Research Part C: Emerging Technologies*, 65:128–143, 2016.

[10] Jie Yang, Jing Dong, and Liang Hu. A data-driven optimization-based approach for siting and sizing of electric taxi charging stations. *Transportation Research Part C: Emerging Technologies*, 77:462–477, 2017.

[11] Yu Zheng, Zhao Yang Dong, Yan Xu, Ke Meng, Jun Hua Zhao, and Jing Qiu. Electric vehicle battery charging/swap stations in distribution systems: comparison study and optimal planning. *IEEE Transactions on Power Systems*, 29(1):221–229, 2014.

[12] Zhi-Hong Zhu, Zi-You Gao, Jian-Feng Zheng, and Hao-Ming Du. Charging station location problem of plug-in electric vehicles. *Journal of Transport Geography*, 52:11–22, 2016.

[13] Yongjun Ahn and Hwasoo Yeo. An analytical planning model to estimate the optimal density of charging stations for electric vehicles. *PloS one*, 10(11):e0141307, 2015.

[14] Sung Hoon Chung and Changhyun Kwon. Multi-period planning for electric car charging station locations: A case of korean expressways. *European Journal of Operational Research*, 242(2):677–687, 2015.

[15] Herman Jacobus Vermaak and Kanzumba Kusakana. Design of a photovoltaic–wind charging station for small electric tuk–tuk in dr congo. *Renewable Energy*, 67:40–45, 2014.

[16] Md Shariful Islam, N Mithulananthan, Krischonme Bhumkittipich, and Arthit Sode-Yome. Ev charging station design with pv and energy storage using energy balance analysis. In *Innovative Smart Grid Technologies-Asia (ISGT ASIA), 2015 IEEE*, pages 1–5. IEEE, 2015.

[17] Md Mainul Islam, Hussain Shareef, and Azah Mohamed. Improved approach for electric vehicle rapid charging station placement and sizing using google maps and binary lightning search algorithm. *PloS one*, 12(12):e0189170, 2017.

[18] David Pozo, Enzo E Sauma, and Javier Contreras. A three-level static milp model for generation and transmission expansion planning. *IEEE Transactions on Power Systems*, 28(1):202–210, 2013.

[19] Ehsan Hajipour, Mokhtar Bozorg, and Mahmud Fotuhi-Firuzabad. Stochastic capacity expansion planning of remote microgrids with wind farms and energy storage. *IEEE Transactions on Sustainable Energy*, 6(2):491–498, 2015.

[20] Ting Qiu, Bolun Xu, Yishen Wang, Yury Dvorkin, and Daniel S Kirschen. Stochastic multistage coplanning of transmission expansion and energy storage. *IEEE Transactions on Power Systems*, 32(1):643–651, 2017.

[21] Michal Kaut, Kjetil T Midthun, Adrian S Werner, Asgeir Tomasgard, Lars Hellemo, and Marte Fodstad. Multi-horizon stochastic programming. *Computational Management Science*, 11(1-2):179–193, 2014.

[22] Lars Hellemo, Kjetil Midthun, Asgeir Tomasgard, and Adrian Werner. Natural gas infrastructure design with an operational perspective. *Energy Procedia*, 26:67–73, 2012.

[23] Lars Hellemo, Kjetil Midthun, Asgeir Tomasgard, and Adrian Werner. Multi-stage stochastic programming for natural gas infrastructure design with a production perspective. In *Stochastic Programming: Applications in Finance, Energy, Planning and Logistics*, pages 259–288. World Scientific, 2013.

[24] Hubert Abgottspon. *Hydro power planning: Multi-horizon modeling and its applications*. PhD thesis, 2015.

[25] Hubert Abgottspon and Göran Andersson. Multi-horizon modeling in hydro power planning. *Energy Procedia*, 87:2–10, 2016.

[26] Pernille Seljom and Asgeir Tomasgard. The impact of policy actions and future energy prices on the cost-optimal development of the energy system in norway and sweden. *Energy Policy*, 106:85–102, 2017.

[27] Pernille Seljom and Asgeir Tomasgard. Short-term uncertainty in long-term energy system models - a case study of wind power in denmark. *Energy Economics*, 49:157–167, 2015.

[28] Christian Skar, Gerard Doorman, and Asgeir Tomasgard. The future european power system under a climate policy regime. In *Energy Conference (ENERGYCON), 2014 IEEE International*, pages 318–325. IEEE, 2014.

[29] Paula Rocha, Michal Kaut, and Afzal S Siddiqui. Energy-efficient building retrofits: An assessment of regulatory proposals under uncertainty. *Energy*, 101:278–287, 2016.

[30] Scott B Peterson, JF Whitacre, and Jay Apt. The economics of using plug-in hybrid electric vehicle battery packs for grid storage. *Journal of Power Sources*, 195(8):2377–2384, 2010.

[31] Rodolfo Dufo-López, José L Bernal-Agustín, and José A Domínguez-Navarro. Generation management using batteries in wind farms: Economical and technical analysis for spain. *Energy policy*, 37(1):126–139, 2009.

[32] Ronald M Dell and David Anthony James Rand. *Understanding batteries*. Royal Society of Chemistry, 2001.

[33] Nicholas DiOrio, Aron Dobos, Steven Janzou, Austin Nelson, and Blake Lundstrom. Technoeconomic modeling of battery energy storage in sam. *National Renewable Energy Laboratory (NREL) NREL/TP-6A20–64641*, 2015.

[34] Henrik Bindner, Tom Cronin, Per Lundsager, James F Manwell, Utama Abdulwahid, and Ian Baring-Gould. *Lifetime modelling of lead acid batteries*. 2005.

[35] Robert Spotnitz. Simulation of capacity fade in lithium-ion batteries. *Journal of Power Sources*, 113(1):72–80, 2003.

[36] Cadex Electronics Inc. Series and parallel battery configurations. `http://batteryuniversity.com/learn/article/serial_and_parallel_battery_configurations`. Online; accessed 2017.

[37] Trojan Battery Company. Battery mainteinance. `http://www.trojanbattery.com/tech-support/faq/`. Online; accessed 2017.

[38] Mitsubishi Electric. Mitsubishi electric delivers high-capacity energy-storage system to kyushu electric power's buzen substation. `http://www.mitsubishielectric.com/news/2016/0303-b.html`, 2016. Online; accessed 2017.

[39] Fred Lambert. Tesla quietly brings online its massive biggest in the world 80 mwh powerpack station with southern california edison. `https://electrek.co/2017/01/23/tesla-mira-loma-powerpack-station-southern-california-edison/`, 2017. Online; accessed 2017.

[40] Tom Kenning. Sdg&e and aes complete worlds largest lithium ion battery facility. `https://www.energy-storage.news/news/sdge-and-aes-complete-worlds-largest-lithium-ion-battery-facility`, 2017. Online; accessed 2017.

[41] Yanqing Li, Ling Li, Jing Yong, Yuhai Yao, and Zhiwei Li. Layout planning of electrical vehicle charging stations based on genetic algorithm. In *Electrical Power Systems and Computers*, pages 661–668. Springer, 2011.

[42] Walid El-Khattam, YG Hegazy, and MMA Salama. An integrated distributed generation optimization model for distribution system planning. *IEEE Transactions on Power Systems*, 20(2):1158–1165, 2005.

[43] Thomas Allen Short. *Electric power distribution handbook*. CRC press, 2014.

[44] Mohammad Yazdani-Asrami, Mohammad Mirzaie, and Amir Abbas Shayegani Akmal. No-load loss calculation of distribution transformers supplied by nonsinusoidal voltage using three-dimensional finite element analysis. *Energy*, 50:205–219, 2013.

[45] How harmonic mitigating transformers outperform k-rated transformers. Technical report, Hammond Power Solutions Inc.

[46] Mushfiqur R Sarker, Daniel Julius Olsen, and Miguel A Ortega-Vazquez. Co-optimization of distribution transformer aging and energy arbitrage using electric vehicles. *IEEE Transactions on Smart Grid*, 2016.

[47] Michael Christopher Kuss, Anthony J Markel, William Emanuel Kramer, et al. *Application of Distribution Transformer Thermal Life Models to Electrified Vehicle Charging Loads Using Monte-carlo Method: Preprint*. National Renewable Energy Laboratory, 2011.

[48] Robert B Moran. Guidelines for transformer application designs. `http://ecmweb.com/content/guidelines-transformer-application-designs`, 1999. Online; accessed 2017.

[49] IEEE. Recommended practices and requirements for harmonic control in electrical power systems. 1993.

[50] Pietro Belotti, Pierre Bonami, Matteo Fischetti, Andrea Lodi, Michele Monaci, Amaya Nogales-Gómez, and Domenico Salvagnin. On handling indicator constraints in mixed integer programming. *Computational Optimization and Applications*, 65(3):545–566, 2016.

[51] Solar choice battery performance comparison tool. `https://www.solarchoice.net.au/blog/solar-choice-battery-storage-product-lifespan-comparison-tool?nabe=5824973356924928:0`. Online; accessed 2017.

[52] Jochen Linssen, Peter Stenzel, and Johannes Fleer. Techno-economic analysis of photovoltaic battery systems and the influence of different consumer load profiles. *Applied Energy*, 2015.

[53] Lian Yang, Nengling Tai, Chunju Fan, and Yuanye Meng. Energy regulating and fluctuation stabilizing by air source heat pump and battery energy storage system in microgrid. *Renewable Energy*, 95:202–212, 2016.

[54] Peter Bronski, Jon Creyts, Leia Guccione, Maite Madrazo, James Mandel, Bodhi Rader, Dan Seif, P Lilienthal, J Glassmire, J Abromowitz, et al. The economics of grid defection: When and where distributed solar generation plus storage competes with traditional utility service. *Rocky Mountain Institute*, 2014.

[55] Wesley J Cole, Cara Marcy, Venkat K Krishnan, and Robert Margolis. Utility-scale lithium-ion storage cost projections for use in capacity expansion models. In *North American Power Symposium (NAPS), 2016*, pages 1–6. IEEE, 2016.

[56] Johannes Michael Grothoff. Battery storage for renewables: market status and technology outlook. Technical report, Technical Report January, International Renewable Energy Agency (IRENA), 2015.

[57] ISE Fraunhofer and Agora Energiewende. Current and future cost of photovoltaics; long-term scenarios for market development, system prices and lcoe of utilityscale pv-systems. *Agora Energiewende*, page 82, 2015.

[58] Rick Tidball, Joel Bluestein, Nick Rodriguez, and Stu Knoke. Cost and performance assumptions for modeling electricity generation technologies. *Contract*, 303:275–3000, 2010.

[59] David Feldman, Robert Margolis, Paul Denholm, and Joseph Stekli. Exploring the potential competitiveness of utility-scale photovoltaics plus batteries with concentrating solar power. 2016.

[60] NREL. Pvwatts calculator. `http://pvwatts.nrel.gov/pvwatts.php`. Online; accessed 2017.

[61] Nord Pool. Historical market data for electricity spot hourly price. `http://www.nordpoolspot.com/historical-market-data/`. Online; accessed 2017.

[62] Jesse Leeuwendal. Kraftmarkedsanalyse 2016 - 2030. Master's thesis, University of Twente, 2013.

[63] Gudmund Bartnes og Eirik øysleb øGudmund Bartnes, Jonas Skaare Amundsen. Kraftmarkedsanalyse 2016 - 2030. Technical report, Norges vassdrags- og energidirektorat - NVE, 2017.

[64] Karin Lövebrant Vstermark Vegard Holmefjord Jørgen Aarstad Eirik Tø mte Bø hnsdalen, Ivar Husevåg Dø skeland. Langsiktig markedsanalyse norden og europa 2016 - 2040. Technical report, Statnett, 2016.

[65] Anibal De Almeida, Bruno Santos, and Fernando Martins. Energy-efficient distribution transformers in europe: impact of ecodesign regulation. *Energy Efficiency*, 9(2):401–424, 2016.

[66] Erling Holden Olav Wicken Marianne Ryghaug Knut Holtan Sø rensen Eva Rosenberg, Kari Aamodt Espegren. Censes energy demand projections towards 2050 - reference path. Technical report, Technical Report, ICF Consulting Services, 2015.

[67] Electric vehicles in europe: gearing up for a new phase? Technical report, Amsterdam Roundtable Foundation and McKinsey and Company The Netherlands, 2014.

[68] EV Global. Outlook 2016, beyond one million electric cars. *International Energy Agency: Paris, France*, 2016.

[69] Mark Allington Theoni Versi. Overview of the electric vehicle market and the potential of charge points for demand response. Technical report, Technical Report, ICF Consulting Services, 2016.

[70] ABB. Distribution transformers. `http://new.abb.com/products/transformers/distribution`. Online; accessed 2017.

[71] Ehsan Hajipour, Maryam Mohiti, Nima Farzin, and Mehdi Vakilian. Optimal distribution transformer sizing in a harmonic involved load environment via dynamic programming technique. *Energy*, 120:92–105, 2017.

[72] REN Et samarbeid med SINTEF. Planbok - oppdatert og systematisert planleggingsbok for kraftnettet. `http://www.ren.no/produkter/planbok`. Online; accessed 2017.

[73] S Dutta and TJ Overbye. A clustering based wind farm collector system cable layout design. In *Power and Energy Conference at Illinois (PECI), 2011 IEEE*, pages 1–6. IEEE, 2011.